A Stochastic Techno-Economic Framework for Hydrogen-based Maritime Decarbonisation under Market and Policy Uncertainty

Li Chin Law [1,5,*], Osman Gungen[3], Selim Gungen[3], John Cooper[4] and Epaminondas Mastorakos [1,2,*]

[1] Cambridge Centre for Advanced Research and Education in Singapore (CARES), CREATE Tower, 1 Create Way, Singapore
[2] Engineering Department, University of Cambridge, Cambridge, United Kingdom
[3] Güngen Denizcilik ve Ticaret A.Ş., Gazi Osman Pasa, Ankara, Turkey
[4] Metavasi Strategies Limited, London, United Kingdom
[5] EMICAST Private Limited, CREATE Tower, 1 Create Way, Singapore

* Correspondence: lcl38@cam.ac.uk (L.C.L.); em257@eng.cam.ac.uk (E.M.)
Tel.: +65-88852052 (L.C.L.)

Abstract

Maritime decarbonisation pathways are subject to substantial uncertainty arising from volatile fuel markets and evolving regulatory frameworks. This study develops a stochastic techno-economic framework to evaluate the lifecycle cost competitiveness of hydrogen-based propulsion systems under combined market and policy uncertainty. The framework integrates Monte Carlo-based stochastic price uncertainty with scenario-conditioned policy uncertainty, capturing variability in key cost drivers including CAPEX, fuel price, CO_2 value, EU ETS, FuelEU Maritime, and IMO GFI mechanisms. Two hydrogen pathways, namely onboard hydrogen production using steam methane reforming with carbon capture (HPU) and green hydrogen bunkering (Green H_2), are assessed against a conventional oil-fuelled reference ship (RefShip) over the 2030–2050 period. Results show that HPU exhibits strong policy sensitivity and becomes increasingly competitive under supportive policy conditions, whereas Green H_2 competitiveness remains constrained by hydrogen fuel cost. The median net lifecycle cost ratio relative to RefShip, **R**, is in the range **0.24–0.68** for the hydrogen pathways. Excluding FuelEU Maritime and IMO GFI surplus-credit revenues increases the median gross cost ratio to **R = 0.65–0.90** for HPU and approximately **R = ~0.8** for Green H_2. While HPU retains only a small probability of exceeding RefShip costs under Conservative and Moderate policy scenarios, this probability becomes negligible under Optimistic and Policy-Optimal scenarios. Green H_2, however, maintains probability of being more expensive than RefShip across all policy scenarios due to the dominant contribution of hydrogen fuel expenditure. Threshold analysis demonstrates that both pathways remain economically favourable relative to RefShip at EUA prices below **~100 €/tCO₂**, hydrogen price below **~$5.8/kg H₂**, and CO_2 offloading costs below **~$300/tCO₂**.

The results demonstrate the importance of stochastic assessment for capturing long-term investment risk and policy uncertainty, highlighting the value of the proposed framework for risk-informed maritime decarbonisation planning.

***Keywords*—** maritime, hydrogen propulsion, onboard carbon capture, LNG-fuelled ship, ship decarbonisation, economic, Monte Carlo risk analysis

AE	Auxiliary engine
CAPEX	Capital expenditure
CCGT	Combined cycle gas turbine
CCS	Carbon capture and storage system
CII	Carbon Intensity Indicator
CO_2	Carbon dioxide
D	Voyage distance
DWT	Deadweight Tonnage
EU	European Union
EUA	EU allowances
EU ETS	EU Emissions Trading System
gBm	Geometric Brownian motion
GFI	Greenhouse Gas Fuel Intensity
GHG	Greenhouse Gas
GHGIE	Greenhouse gas intensity of energy
H_2	Hydrogen
HPU	Hydrogen production unit
HTWGS	High temperature water gas shift
IMO	International Maritime Organization
LCOH	Levelised cost of hydrogen
LNG	Liquefied natural gas
Log-OU	logarithmic Ornstein–Uhlenbeck
LTWGS	Low temperature water gas shift
MC	Monte Carlo
ME	Main engine
MEPC	Maritime Environment Protection Committee
MGO	Marine Gas Oil
MT	Metric tonnes
N	Sample size of Monte Carlo simulation
OCCS	Onboard carbon capture and storage
OPEX	Operating cost
P10	10^{th} percentile of simulated results
P50	Median (50^{th} percentile) simulated results
P90	90^{th} percentile of simulated results
PDF	Probability density distributions
PreCCS	Pre-combustion carbon capture
PSA	Pressure swing adsorption
R	Cost ratio
SMR	Steam methane reformer
VLSFO	Very Low Sulfur Fuel Oil
WGS	Water gas shift reaction

1. INTRODUCTION

To reduce ship emissions, the maritime sector must undergo a rapid transition partly driven by increasingly stringent decarbonisation regulations. Regulatory frameworks such as the International Maritime Organization (IMO) greenhouse gas strategy, the European Union Emissions Trading System (EU ETS), and FuelEU Maritime are significantly reshaping operational and investment decisions across the shipping industry. In response, a wide range of low-carbon propulsion pathways, including alternative fuels and onboard carbon capture technologies (OCCS), are being actively explored.

Among these, hydrogen is widely regarded as a promising zero-carbon fuel. However, its practical deployment in shipping remains constrained by technical and economic challenges [1]. The low volumetric energy density of hydrogen can reduce cargo capacity for long-voyage vessels [2], while issues such as leakage and boil-off require advanced storage systems with high capital cost [3]. In addition, green hydrogen supply chain and bunkering facilities are still under development [4], with high costs associated with electrolysis and renewable electricity and transportation [5]. Reported historical hydrogen sale prices vary with time, ranging from \$5.5 to \$11/kg H_2 from 2022 to 2026 [6]. The levelised cost of hydrogen (LCOH) is reported to depend strongly on production pathways and cost of renewable electricity [7] [8]. In comparison, conventional marine fuels such as VLSFO remain substantially cheaper (< \$1000 per MT based on Rotterdam price indices between 2023 and 2026 [9]), leading to concerns over the economic viability of direct hydrogen adoption. Additional concerns with hydrogen bunkering involve the high cost of liquefying it and the potential of leaks, which can negate some of the environmental benefit because hydrogen has significant greenhouse gas potential if accidentally released [10].

An alternative approach is onboard hydrogen production using fossil-based fuels, typically methane, combined with carbon capture. Previous studies published in Ref. [11] have demonstrated the thermodynamic feasibility of onboard natural gas reforming with pre-combustion carbon capture (PreCCS), enabling low-carbon hydrogen production for ship propulsion. Further integration with combined-cycle gas turbine (CCGT) systems has been shown to improve overall efficiency [12]. In such configurations, liquefied natural gas (LNG) is converted onboard into hydrogen, while CO_2 is captured as a by-product, thereby reducing emissions while mitigating hydrogen storage challenges. Despite promising technical reliability level, the economic viability of onboard hydrogen production-based systems remains dependent on several uncertain factors including feedstock fuel price volatility, evolving carbon markets, and dynamic regulatory frameworks, which can introduce considerable uncertainty into long-term investment decisions.

Existing techno-economic analyses have evaluated hydrogen-fuelled vessels and hydrogen transport systems [13], with some studies incorporating emission penalties to enable comparison with conventional fuel-oil-based vessels [14]. Policy-oriented research has also highlighted the importance of regulatory

support in accelerating low-carbon ship investments [15]. However, most studies rely on deterministic assumptions, typically based on fixed fuel prices and static policy conditions.

In many techno-economic studies, the cost parameters such as CAPEX and fuel prices are assumed with a fixed value [16]. Such assumptions overlook the inherent volatility associated with technological development, market dynamics, and policy uncertainty, potentially leading to underestimation of financial risk and misrepresentation of technology competitiveness. To address price variability, several studies have applied stochastic modelling approaches. For example, Hoejin and Heesung [17] modelled EU allowances (EUA) prices using geometric Brownian motion (gBm), while fuel prices such as LNG and MGO were represented using mean-reverting Ornstein-Uhlenbeck processes. Other studies have adopted simplified projections, such as linear price escalation for EUA and fuels [18]. Monte Carlo simulation has also been applied to evaluate sensitivity of key economic variables, including discount rates [19], fuel costs, and carbon prices [20].

In decarbonisation, the cost of carbon and policies such as EU ETS, FuelEU Maritime, and the IMO Greenhouse Gas Fuel Intensity (GFI) framework introduce further economic complexity through penalties and surplus credit trading [21]. While penalty rates are prescribed by regulation, the future prices of surplus compliance credits are expected to be determined by market transactions between compliant and non-compliant ships and therefore remain highly uncertain [22] [23]. Lloyd's Register has highlighted that the transaction of Surplus Units from an over compliant ship to an under compliant ship will be governed by private contract. Consequently, the Remedial Unit price, such as \$380/ton CO_2eq under IMO GFI framework is expected to represent the upper limit for the price of a Surplus Unit [24], although its actual trading price could be lower. However, these policy variables are usually being treated as fixed inputs and are rarely modelled as dynamic and uncertain regulatory mechanisms, limiting the ability of current analyses to capture the combined impact of market and regulatory uncertainty on investment risk. Recent studies have further shown that surplus credit prices can influence the financial feasibility of low-emission technologies [25] [26], highlighting the importance of explicitly representing this uncertainty in long-term investment assessment.

To address these gaps, this study develops a stochastic techno-economic framework to evaluate maritime decarbonisation pathways under combined market and regulatory uncertainty. The framework integrates time-correlated fuel and carbon price modelling with scenario-conditioned policy pathways within a unified financial model. A Monte Carlo structure is introduced to represent baseline market uncertainty and policy-driven variability, recognising that stochastic market evolution alone is insufficient to evaluate policy-driven cost parameters (such as surplus credits), whose values depend on future regulatory ambition and market participation and therefore require separate stochastic modelling across alternative policy scenarios. This enabling a more comprehensive assessment of investment risk and technology competitiveness under

evolving market and regulatory conditions.

The key contributions of this study are as follows:

1. **Integrated techno-economic model development**: Construct an integrated techno-economic model for lifecycle cost assessment.
2. **Scenario-conditioned Monte Carlo structure:** Introduces a novel structure coupling baseline market uncertainty and scenario-conditioned policy uncertainty for fuel prices, carbon prices, and regulatory variables.
3. **Dynamic policy representation:** Models regulatory variables (e.g., EU ETS, CO_2 value, FuelEU, GFI) as stochastic, time-evolving variables.
4. **Risk-based economic evaluation:** Uses probabilistic metrics (P10, P50, P90, distributions) to quantify investment risk and economic robustness.

In this study, the framework is demonstrated using hydrogen-fuelled vessel concepts: one employing green hydrogen bunkering (denoted as Green H_2) and another identical vessel equipped with hydrogen production unit (HPU) and carbon capture (denoted as HPU). However, the methodology is generalisable and can potentially be applied to other ship types and low-carbon fuel pathways, including ammonia, methanol and biofuels. By providing probabilistic cost distributions and risk-based insights, the framework supports robust and uncertainty-aware investment decision-making in the maritime sector.

In short, this study proposes a stochastic techno-economic framework that enables risk-informed investment decision-making under combined market and regulatory uncertainty. By embedding policy-driven stochastic dynamics within a hierarchical Monte Carlo structure, the framework captures the propagation of uncertainty into long-term cost outcomes. The remainder of this paper is structured as follows: Section 2 presents the research methodology, Section 3 discusses results and key findings, and Section 4 provides conclusions and recommendations.

2. METHODOLOGY

2.1. Research approach

Figure 1 presents the proposed stochastic techno-economic framework for lifecycle cost assessment of low-carbon ship propulsion pathways under market and regulatory uncertainty. The framework consists of four main components: (i) ship modelling, (ii) ship-level techno-economic modelling, (iii) stochastic uncertainty modelling with Monte Carlo simulation, and (iv) probabilistic techno-economic and risk evaluation model.

First, the reference ship and alternative propulsion configurations are simulated based on a defined ship route to determine voyage distance, engine performance, fuel consumption and emissions characteristics. These outputs are subsequently used to estimate the required capacity of onboard hydrogen production units and associated low-carbon technologies, which influence both CAPEX and OPEX.

Second, a ship-level techno-economic model is developed to calculate annual and cumulative lifecycle costs. The model incorporates fuel cost, annualised CAPEX, maintenance cost, CO_2 offloading cost, EU ETS cost, FuelEU Maritime penalty or surplus, and IMO GFI penalty or surplus. Third, uncertainty is introduced through a Monte Carlo framework representing stochastic market and policy uncertainty across key cost drivers. Finally, the stochastic market and policy models are integrated into the techno-economic model to iteratively simulate the lifecycle cost performance of selected pathways. This enables uncertainty propagation, comparative assessment, and probabilistic risk assessment across alternative propulsion configurations.

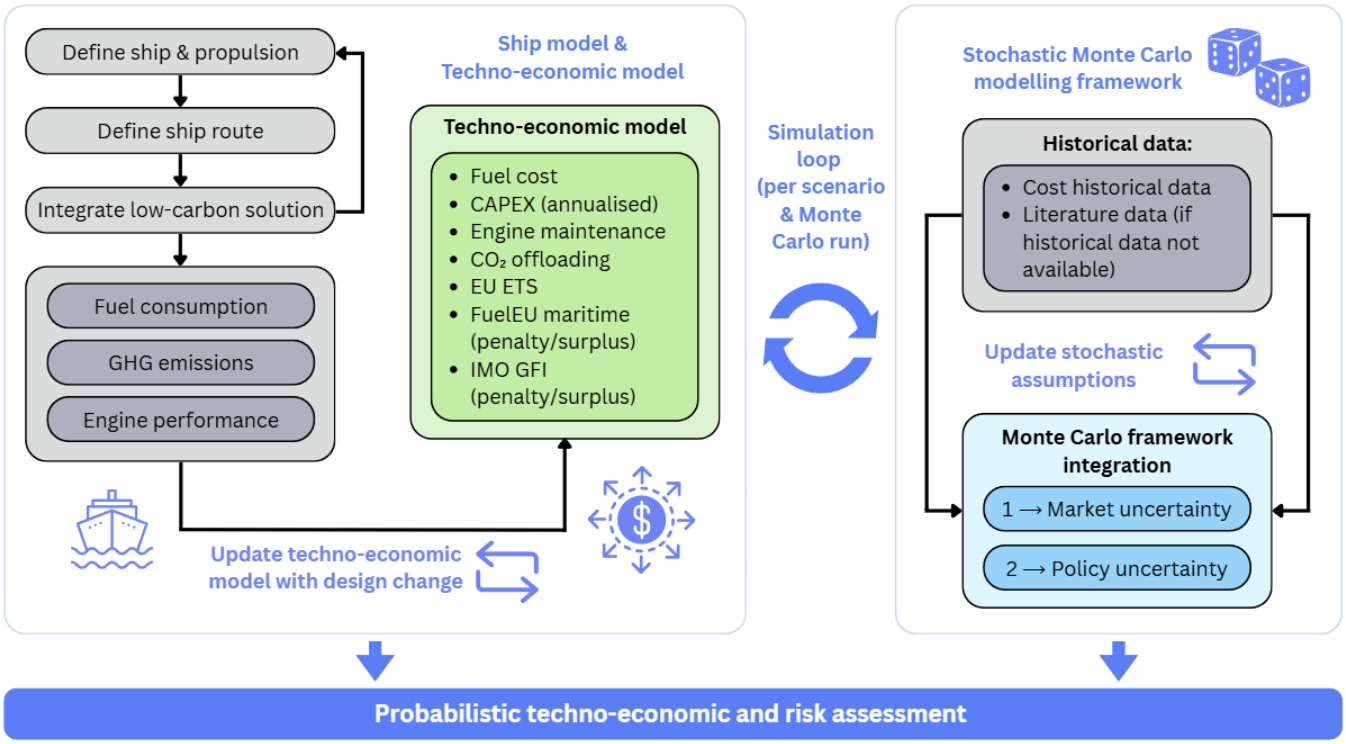


Figure 1. Overall stochastic techno-economic assessment framework developed for lifecycle cost and risk evaluation of low-carbon ship propulsion pathways. The framework integrates ship modelling, techno-economic analysis, a stochastic Monte Carlo framework and risk assessment model to evaluate lifecycle cost competitiveness under market and policy uncertainty. Iterative simulation loops enable probabilistic risk assessment across alternative propulsion configurations.

2.2. Ship model

2.2.1 Ship particulars

The reference ship is a 93,000-deadweight tonnage (DWT) vessel fuelled by marine gas oil (MGO), representing the conventional baseline configuration (denoted as RefShip, Figure 2 (a)). Two alternative low-carbon propulsion pathways are evaluated against the reference case: (i) direct green hydrogen-bunkering (Green H_2, Figure 2 (b)) and (ii) onboard hydrogen production using steam methane reforming system integrated with pre-combustion carbon capture (HPU, Figure 2 (c)). Figure 2 illustrates the conceptual arrangement in which the green hydrogen storage tanks and the hydrogen production unit are primarily located in above-deck spaces to minimise the loss of cargo capacity [27] [25]. However, potential cargo-capacity impacts associated with equipment weight and volume, weight distribution, and ship stability require detailed assessment and have not been evaluated in the present study.

For the direct hydrogen bunkering case, based on the reported boil-off rate of ~1.063%/day [3], all hydrogen boil-off gas would be fully utilised onboard upon vaporisation to meet the daily fuel consumption rate [28], eliminating the need for additional reliquefaction energy. Consequently, the useful propulsion energy demand is assumed to be equivalent to that of the RefShip case. In terms of lifecycle emission, according to the Renewable Energy Directive (EU) 2018/2001 (RED II), renewable hydrogen must achieve at least 70% GHG savings from fossil fuel comparator of 94 gCO_2eq/MJ, corresponds to a maximum emission intensity of 28.2 gCO_2eq/MJ. However, the actual emission factor of Green H_2 can vary with sources of renewable energy. The National Renewable Energy Laboratory [29] and a literature review covering 153 lifecycle studies on wind and solar energy [30] reported electricity-generation lifecycle emissions of up to 218 gCO_{2eq}/kWh (60.6 gCO_{2eq}/MJ) for solar and 364.8 gCO_{2eq}/kWh (101.3 gCO_{2eq}/MJ) for wind energy. Law et al. [31] reported the energy consumed per MJ of green H_2 produced to be 0.66 including energy demand for electrolyser and compression. Consequently, using electricity source of 50 gCO_{2eq}/kWh could produce green hydrogen of ~23 gCO_2eq/MJ, equivalent to ~ 2.8 gCO_2/kgH_2 [32].

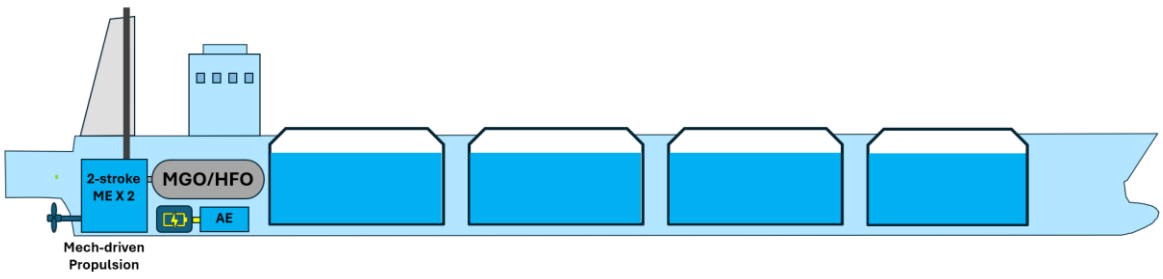
For the onboard hydrogen production pathway, LNG is converted into hydrogen onboard using a hydrogen production unit (HPU) integrated with carbon capture technology. Comparative assessment between hydrogen production technologies was conducted in Ref. [11] and a steam methane reformer (SMR) due to its superior energy efficiency is selected for the present study. The performance of an SMR is simulated and optimised using Aspen HYSYS. Here, the steam to fuel ratio (S/C) is controlled to achieve optimal conversion and hydrogen production. Waste heat downstream the reformer and Water-Gas Shift (WGS) reactors is recycled to generate superheated steam. In addition, part of the produced hydrogen is fed back into the reformer's furnace to generate heat for the reformer to maximise reduction in the overall greenhouse gas (GHG) footprint of the system. The simplified process flow diagram and Aspen model of the HPU are

presented in Appendix A (Figure A1), and the inputs and results obtained from HPU optimisation are summarised in Appendix A (Table A2, Table A3). The performance of the ship integrated with the Aspen-designed HPU is assessed based on the approach outlined in Appendix B, and the findings simulated outputs is summarised in Table 1, the overall energy penalty of HPU is simulated to be ~21% to achieve net CO_2 reduction of ~85%. Table 1 also shows the key operational and emission characteristics of the propulsion pathways investigated in this study.

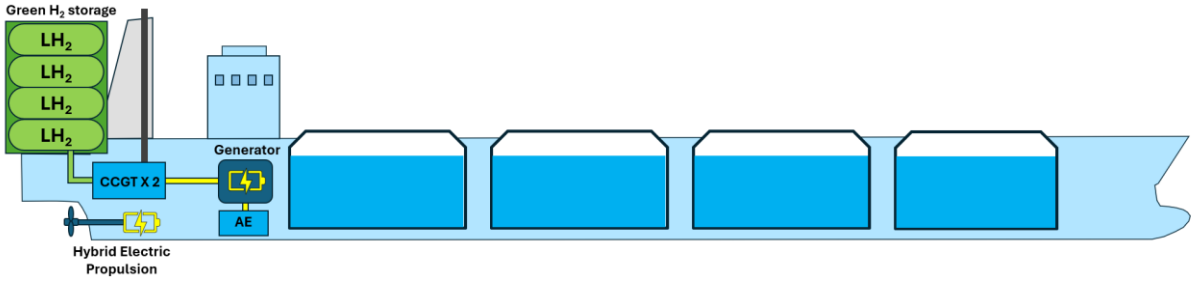
In terms of propulsion technology, hydrogen-fuelled reciprocating engines are currently at a relatively low technology readiness level. In contrast, CCGT systems capable of operating on 100% hydrogen or hydrogen-natural gas blends are already commercially available for power generation [33] [34]. Hence, both Green H_2 and HPU pathways considered in this study employ electric propulsion with CCGT-based electricity production. Although large-scale CCGT plants can achieve higher efficiencies than conventional marine two-stroke engines, however, a common net efficiency of approximately 50% is adopted in this study considering the performance of marine-scale hydrogen CCGT[12] [34] [35]. This assumption is consistent with reported efficiencies of approximately 50% for low-speed two-stroke main engines [36] and 50-51.6% for offshore or marine CCGT systems [35] [12]. The use of a common representative efficiency also avoids introducing additional uncertainty associated with future propulsion-system performance and enables a more direct comparison of fuel and policy effects across the evaluated pathways.

The vessels are assumed to operate on repeated round trips between Corpus Christi and Rotterdam over the 2030–2050 assessment horizon. Under FuelEU Maritime regulation, voyages between EU/EEA and non-EU/EEA ports are subjected to 50% attribution of relevant emissions. Accordingly, the remaining 50% of emissions is assumed to be regulated under the IMO GFI framework for penalty or surplus-credit calculations.

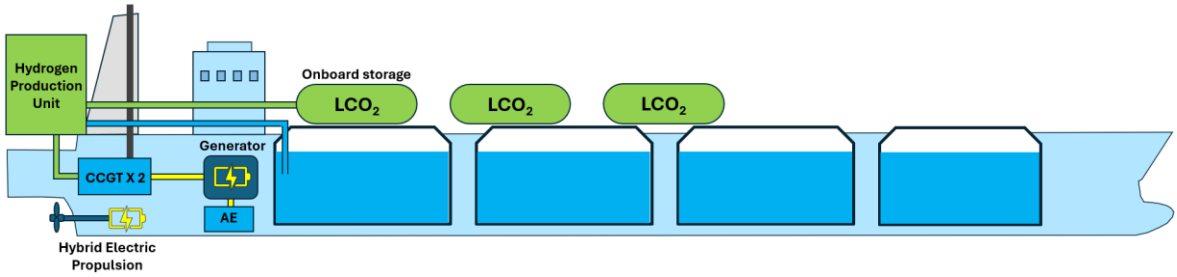
Voyage distance (D) is estimated using the haversine formula (Equation 1) [37], where R is the Earth radius, ϕ is latitude in radians, and λ is longitude in radians. Based on the port coordinates, the one-way voyage distance is estimated at ~5,150 nautical miles (nm), corresponding to ~10,300 nm per round trip. Assuming 10.5 round trips annually, the vessel travels approximately 108,000 nm per year.



(a)



(b)



(c)

Figure 2. Conceptual propulsion configurations evaluated in this study: (a) reference MGO-fuelled mechanically driven propulsion system (RefShip); (b) direct green hydrogen bunkering with electric propulsion (Green H_2); and (c) onboard hydrogen production unit (HPU) using steam methane reforming integrated with pre-combustion carbon capture and electric propulsion. The alternative configurations conceptually utilise above-deck space for hydrogen storage or hydrogen production equipment to minimise cargo capacity loss; detailed ship-integration feasibility is beyond the scope of the present study.

$$D = 2Rsin^{-1}\left(\sqrt{sin^2\left(\frac{\phi_2-\phi_1}{2}\right)+\cos(\phi_1)\cdot\cos(\phi_2)\cdot sin^2\left(\frac{\lambda_2-\lambda_1}{2}\right)}\right) \quad (1)$$

Table 1. Summary of key operational, fuel-consumption, and emission characteristics of the reference oil-fuelled ship (RefShip), Green H_2 pathway, and onboard hydrogen production pathway using HPU with carbon capture. The table shows energy demand, fuel consumption, TTW and WTT emissions, and CO_2 capture performance for the selected propulsion configuration. The values provided is used as inputs for the deterministic techno-economic and stochastic lifecycle cost assessment.

Trip number	*Reference ship (oil)*	*Green H_2*	*HPU*	*Data source*
Fuel for propulsion	MGO	H_2	H_2 (produced onboard)	-
Lower heating value (MJ/kg)	42.7	120	50 (for HPU feedstock)	[38]
CO_2 emission factor, $C_{f,CO2}$ ($gCO_2/gFuel$)	3.206	0	2.750	[38]
CH_4 emission factor, $C_{f,CH4}$ ($gCH_4/gFuel$)	0.00005	0	0	[38]
N_2O emission factor, $C_{f,N2O}$ ($gN_2O/gFuel$)	0.00018	0	0.00011	[38]
TTW (gCO_2eq/MJ)	76.2	0	55.6 (for HPU feedstock)	[1] Calculated
WTT (gCO_2eq/MJ)	14.4	23.1	18.5 (for HPU feedstock)	[38]
Main engine (ME)	2-stroke engine 13MW (2-stroke ME X 2)	CCGT 16MW (CCGT X 2)	CCGT 16MW (CCGT X 2)	Assumption, *Figure 2*
CAPEX of ME or CCGT ($/kW)	500 ± 15%	1200 ± 50%	1200 ± 50%	[39]

CAPEX of HPU ($/kg H_2)	-	-	0.5 ± 50%	[40]
MGO consumed (ton/y)	19,501	0	23.0	[2] Simulated
LNG consumed (ton/y)	0	0	21,174	[2] Simulated
H2 consumed (ton/y)	0	6,939	0	[2] Simulated
Annual energy (MJ/y)	832,712,391	832,712,391	1,059,681,786	[2] Simulated
CO_2 emitted (t/y)	62,522	0	9,598	[2] Simulated
CO_2eq emitted (t/y)	63,479	0	10,870	[2] Simulated
WTW CO_2eq emitted (t/y)	75,470	19,202	30,477	[2] Simulated
CO_2 captured (t/y)	0	0	48,814	[2] Simulated
ME or CCGT hours	15,389	9,202	8,150	[2] Simulated
Maintenance cost ME or CCGT ($/MWh)	2.5 % of CAPEX/year [39]	4 % of CAPEX/year [39]	4 % of CAPEX/year [39]	Assumption
CII (gCO_2/dwt.nm)	6.19	0	0.95	[2] Calculated
WTW GFI (gCO_2eq/MJ)	90.63	23.06	28.8	[2] Calculated

Note: 1. The TTW emission factor in the unit of gCO_2eq/MJ fuel is estimated by multiplying the TTW emission factors $C_{f,CO2}$, $C_{f,CH4,}$ and $C_{f,N2O}$ with their 100-year global warming potential (GWP) factor of 1 for CO_2, 28 for CH_4, and 265 for N_2O, in accordance with IMO Resolution MEPC.376(80) [41]. 2. The values were obtained from ship performance simulation, which has been conducted accordingly to the methodology outlines in Appendix B.

2.3. Techno-economic model

The total annual cost is defined as:

$$C_{total,t} = C_{CAPEX,t} + C_{fuel,t} + C_{m,t} + C_{CO2,t} + C_{ETS,t} + C_{FuelEU,t} + C_{GFI,t} \quad (2)$$

Where:

- C_{CAPEX} represents the annualised capital expenditure associated with the respective main propulsion system (e.g., convention two-stroke ME or CCGT), and HPU plant (including the hydrogen production unit and CO_2 separation and storage systems).
- C_{fuel} is fuel-related operating cost
- C_m denotes engine and HPU technology maintenance cost
- C_{CO2} is captured CO_2 handling and offloading cost
- C_{ETS} represents EU ETS compliance or EUA cost
- C_{FuelEU} and C_{GFI} represent the penalty or surplus-credit contributions associated with FuelEU Maritime and IMO GFI regulations, respectively.

When surplus credits are included, the resulting annual cost is referred to as the *net annual cost*. Conversely, exclusion of surplus-credit revenues yields the *gross annual cost*, representing the underlying operational and compliance expenditure without policy-credit benefits.

The cumulative lifecycle cost over the assessment horizon T(2030–2050) is calculated as:

$$C_{total,cum} = \sum_{t=2030}^{2050} C_{total,t} \quad (3)$$

2.4. Stochastic modelling framework

Uncertainty modelling is implemented using Monte Carlo framework, as illustrated in Figure 3. In the upper layer (U), baseline stochastic uncertainty is represented through both market-related variables and project-cost variables. Market-related variables included in Equation (2), namely C_{fuel}, C_{CO2}, C_{ETS}, C_{FuelEU} and C_{GFI} are simulated to generate monthly price trajectories, which are subsequently aggregated into annual average price paths over the assessment period. In contrast, CAPEX uncertainty is represented using technology-specific ranges: ±50% for technologies with greater uncertainty associated with their ship-base application and system integration, such as the HPU and CCGT, and ±15% for mature technologies, such as two-stroke marine engines [42]. CAPEX uncertainty is sampled once per Monte Carlo simulation, and annualised over the project lifetime, as CAPEX is treated as a fixed project investment rather than a yearly fluctuating variable. Maintenance cost is represented as a fixed annual fraction of the sampled CAPEX and is therefore recalculated for each Monte Carlo realisation. Consequently, maintenance cost varies between Monte Carlo realisations but remains constant throughout the project lifetime within each realisation. Nevertheless, these parameters are expected to contribute less significantly to the total lifecycle cost compared with OPEX [40].

Building on the baseline uncertainty generated in the upper layer, the lower layer (L) conditions the policy-sensitive variables accordingly to alternative regulatory scenario. As shown in Figure 3, policy-sensitive variables including EUA prices, CO_2 offloading value or handling cost, FuelEU surplus-credit price, and IMO GFI surplus-credit price are adjusted according to four regulatory scenarios: Conservative, Moderate, Optimistic, and Policy-Optimal.

The stochastic market and policy variables are subsequently integrated into the techno-economic model to recalculate lifecycle costs for each Monte Carlo realisation and policy scenario. This process generates probabilistic distributions of both total lifecycle cost and individual cost components. The resulting outputs are used to evaluate economic risk, and policy sensitivity using P10/P50/P90 statistics, lifecycle cost ratios (R) relative to the reference ship, and competitiveness threshold analysis under varying fuel-market and regulatory conditions. These probabilistic outputs provide quantitative insights into pathway competitiveness, investment risk, and the influence of future policy stringency on maritime decarbonisation strategies.

In summary, stochastic trajectories for LNG, MGO and EUA prices are generated using historically calibrated statistical models, while CO_2 value, FuelEU credits, GFI credits, CAPEX and maintenance assumptions are represented using literature-derived uncertainty distributions. The resulting annual trajectories and cost samples are propagated through the techno-economic model for each Monte Carlo realisation and policy scenario. Outputs from all realisations are subsequently used to construct probability

density functions, quantify economic risk, evaluate lifecycle cost ratios, and perform threshold analyses for comparative assessment of the alternative ship architectures.

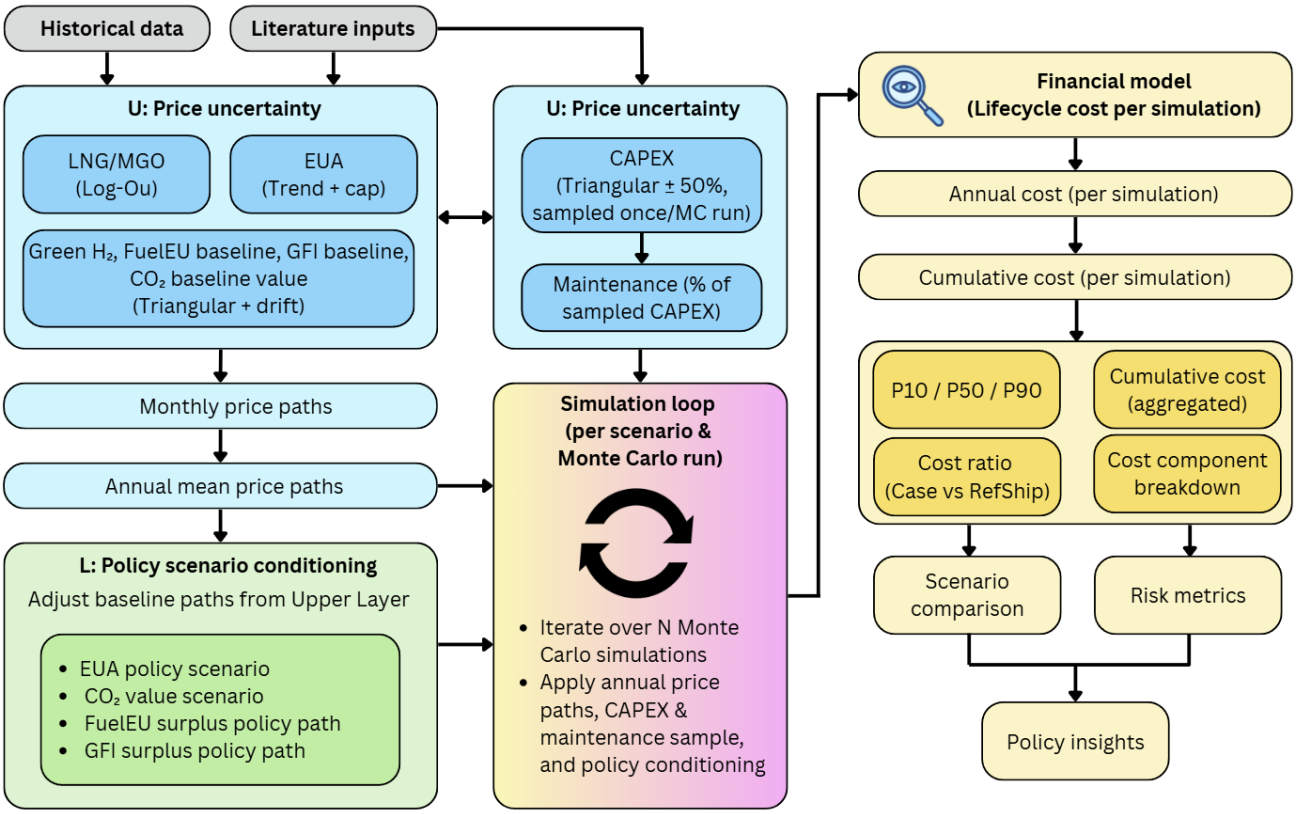


Figure 3. Schematic of the Monte Carlo framework for stochastic techno-economic assessment. In the upper layer (U), baseline stochastic trajectories are generated for fuel prices, EUA prices, FuelEU credit values, GFI credit values, and CO_2 value using historical calibration and literature-derived distributions. Project-cost uncertainty is represented through CAPEX sampled once per Monte Carlo realization using a triangular distribution (±50% or ±15% of the base value depending on technology maturity), while maintenance cost is calculated as a fixed percentage of CAPEX. In the lower layer (L), baseline trajectories are conditionally adjusted according to regulatory scenarios, including EUA policy assumptions, CO_2 value scenarios, and FuelEU/GFI surplus-credit pathways. The resulting inputs are propagated through the lifecycle financial model to generate probabilistic cost distributions, competitiveness metrics, and policy insights.

2.4.1 Upper layer: Market uncertainty

The upper layer generates baseline stochastic market price paths. With sufficient historical data, the LNG and MGO prices are modelled using a logarithmic Ornstein–Uhlenbeck (Log-OU) process. As shown in Equation (4), the random Brownian motion component (dW_t) is introduced to model the stochastic market fluctuations [43] [44] [45]. In this study, the logarithmic approach is adopted instead of classical OU process to ensure that the projected price remain positive [46].

For mature commodities such as LNG and MGO, prices are assumed to fluctuate around the long-run equilibrium level (X_{eq}). The X_{eq}, mean-reverting rate (κ), and volatility (σ) are calibrated from the available historical Rotterdam fuel price series obtained from Ship & Bunker [47], these findings are summarised in Table 2. It is important to note that the calibrated parameters are sensitive towards historical dataset. For example, the historical period between March and May 2026 reflected temporary fuel-price spikes associated with abnormal bunker market conditions [48] [49]. Inclusion of the historical data covering this period introduces upward bias in the estimated long-term equilibrium price and distorts the mean reverting rate and volatility of LNG and MGO. However, the inclusion is reasonable to reflect realistic bunker-market conditions and temporary fuel-price disruptions that may occur.

$$d \ln X_t = \kappa \left(\ln X_{eq} - \ln X_t \right) dt + \sigma dW_t \tag{4}$$

The continuous-time process is discretised using the Euler–Maruyama approximation for monthly simulations, given as Equation (5). This Log-OU differential equation is used for prediction of LNG and MGO fuel prices:

$$\ln X_t = \ln X_{t-1} + \kappa \left(\ln X_{eq} - \ln X_{t-1} \right) \Delta t + \sigma \sqrt{\Delta t} z_t \tag{5}$$

where X_t is the price at time t, X_{eq} is the long-run equilibrium level of fuel price, κ is the annual mean reversion speed, Δt is 1/12 which represents monthly timesteps, σ is the volatility calibrated from historical fuel prices, and $z_t \sim N(0,1)$ is a random number drawn from a standard normal distribution [50].

EUA prices are represented using a log-trend stochastic model. The EUA price is modelled differently assuming that is designed to increase over time to encourage the adoption of carbon reduction measures. Hence, EUA is model using a drift-based stochastic process:

$$d \ln X_t = \mu dt + \sigma dW_t \tag{6}$$

where drift (μ) and volatility (σ) are included. In addition, floor and cap constraints (X_{floor} and X_{cap}) are included to reflect the long-term policy-driven trend in carbon prices while preventing unrealistic values. The EUA's X_{floor} and X_{cap} are set at €50 and €250 per ton of CO_2eq [51], respectively.

$$X_{\text{floor}} \leq X_t \leq X_{\text{cap}} \tag{7}$$

For alternative fuels without sufficiently long historical price series, such as green hydrogen in this study, annual price paths are generated using triangular distributions ($X_{\min}, X_{\text{mode}}, X_{\max}$) with optional drift ($\mu$) and volatility ($\sigma$). Triangular distribution is adopted because it provides a transparent representation of

uncertainty when empirical data are limited. In contrast, the PERT distribution assumes a smoother probability distribution with greater weight around the most-likely value [52], while Beta distribution requires additional assumptions regarding the underlying distribution shape that cannot be robustly justified with the current available data [53]. For future study, the same principle could potentially be applied for renewable ammonia, renewable methanol, and biofuel. The $X_{\min}, X_{\text{mode}}, and\ X_{\max}$ are represented by the minimum, average and maximum prices for the alternative fuels. The data are obtained from the literature, as summarised in

Table 2.

$$X_0 \sim \text{Triangular}(X_{\min}, X_{\text{mode}}, X_{\max}) \tag{8}$$

$$X_t = X_{t-1}\exp\left[\left(\mu - \frac{1}{2}\sigma^2\right) + \sigma z_t\right] \tag{9}$$

where z_t is a random number drawn from a standard normal distribution (mean 0, standard deviation 1), and the volatility (σ) provides the magnitude of considered volatility. The exponential formulation ensures strictly positive fuel prices, while the variance correction term ($-\frac{1}{2}\sigma^2$) prevents upward bias in the projected prices.

In addition to alternative fuel prices, Equation 8 is also used to model uncertainty in the value of captured CO_2 (denoted as C_{CO2}). Since long-term historical market data for CO_2 offloading are limited, annual CO_2 cost paths are also generated using bounded triangular distributions. Two regimes are considered: a disposal-only regime, where captured CO_2 represents a positive cost to the shipowner, and a CO_2 market regime, where captured CO_2 may have neutral or negative net cost due to potential utilisation or credit value [54]. Negative values therefore indicate revenue. The initial annual value is sampled from the relevant triangular distribution and subsequently evolved over time using a stochastic escalation factor with drift and volatility.

The method of modelling and the assumptions applied for the key parameters in uncertainty modelling is summarised in

Table 2. All cost parameters including LNG, MGO, green H_2, CO_2 offload value, and EUA price paths are simulated with sample sizes (N) ranging from N = 1,000 to N = 6,000. A convergence assessment is then performed by comparing the estimated cumulative lifecycle cost distributions in order to determine an appropriate sample size for this study.

Table 2. The upper layer stochastic input parameters. Parameters κ (mean reversion rate), X_{eq} (long-run equilibrium price), and σ (volatility) for LNG and MGO were calibrated from historical prices. For EUA, drift (μ) and volatility (σ) were calibrated from historical log-price changes, and bounded by a floor (X_{floor}) and cap (X_{cap}). For variables without sufficiently long historical price series, bounded triangular distributions ($X_{min}, X_{mode}, X_{max}$) with annual drift and volatility were used.

Variable	***Model***	***Data / basis***	***Key parameters used to model uncertainty***

LNG price ($/MT)	Log-OU	Historical Rotterdam LNG prices [55]	X_0 = latest LNG price; $\Delta t = \frac{1}{12}$ Calibrated parameters: X_{eq} = \$772/MT; $\kappa = 3.23y^{-1}$ [46]; $\sigma = 0.346$
MGO price ($/MT)	Log-OU	Historical Rotterdam MGO prices [55]	X_0 = latest MGO price; $\Delta t = \frac{1}{12}$ Calibrated parameters: X_{eq} = \$892/MT; $\kappa = 1.12y^{-1}$; $\sigma = 0.384$
[2] *EUA price ($/t)*	Log-trend + floor/cap	Historical EUA prices	X_0 = latest EUA price; $\mu = 0.05$; $\sigma = 1.18$ is calibrated from historical price; X_{floor} = 50 €/tCO₂ [56]; X_{cap} = 250 €/tCO₂ [51]
[3] *Captured CO_2 value ($/t CO_2)*	Two-regime triangular + escalation	Literature / assumed ranges	Disposal regime when CO_2 market is not enabled: X_{min} = 75 [57], X_{mode} = 150 [57], X_{max} = 200 USD/tCO₂ [58]; [4] Market regime if CO_2 market is enabled: X_{min} = −35 [54], X_{mode} = 0, X_{max} = 35 USD/tCO₂; $\mu = 0.00$; $\sigma = 0.05$;
[5] *FuelEU surplus price (€/t CO_2)*	Triangular + stochastic escalation	Literature / assumed ranges	X_{min} = 191.7, X_{mode} = 383.4, X_{max} = 575.1 EUR/unit; $\mu = 0.03$; $\sigma = 0.08$; X_{floor} = 100; X_{cap} = 639 EUR/unit [38]
[5] *IMO GFI surplus price (€/t CO_2)*	Triangular + stochastic escalation	Literature / assumed ranges	X_{min} = 114, X_{mode} = 228, X_{max} = 342 USD/unit; $\mu = 0.03$; $\sigma = 0.08$; X_{floor} = 100; X_{cap} = 380 USD/unit [24]
Green H_2 price ($/t)	Triangular + stochastic escalation	Literature ranges	X_{min} = 2000 [59], X_{mode} = 5000 [6], [1] X_{max} = 8000 USD/t ; $\mu = -0.02$; $\sigma = 0.05$; [1] X_{floor} = 1500 USD/t [59]

Note: 1. The upper bound (X_{max}) for green hydrogen price is fixed at 8,000 \$/ton, as prices beyond this level render the considered pathways economically uncompetitive. The lower bound (X_{floor}) for green hydrogen price is set at \$1,500/ton based on the green hydrogen production cost reported by The International Council on Clean Transportation [60]. 2. The EUA floor price (X_{floor}) is assumed to be 50 €/tCO₂ based on historical EUA prices over the past five years, during which EUA prices have consistently remained above 50 €/tCO₂ since May 2021 [56]. The EUA cap (X_{cap}) price is assumed to be 250 €/tCO₂, based on projections indicating EUA prices may reach approximately 200 €/tCO₂ by 2035 [51]. Therefore, for the assessment period of 2035–2050, an upper bound of 250 €/tCO₂ is considered reasonable. 3. According to a report published by the Global CCS Institute in 2025, the cost of CO_2 storage varies depending on storage location and operating conditions, ranging from 5 to 147 USD/tCO₂ [57]. Accordingly, the X_{low} and X_{mode} disposal costs are assumed to be 75 and 150 USD/tCO₂, respectively. A higher bound (X_{max}) of 200 USD/tCO₂ is adopted based on forecasts suggesting that CO_2 storage in the North Sea may become more expensive than previously expected [58]. 4. The potential market value of captured CO_2 is also considered in the assessment. 5. The upper limit of surplus-credit price is assumed to be equal to the corresponding penalty price under the most optimistic (Policy-Optimal) scenarios. This assumption agrees with Lloyd's Register [24] who highlighted that the transfer of surplus units is governed by private contracts, with the maximum price capped at \$380/ton CO2eq (the same as a Remedial Unit), though trades typically occur at a lower rate. Hence, the low, modal, and high surplus-credit prices are assumed to be lower and range between approximately 30%, 60% and 90% of the penalty rate.

2.4.2 Lower layer: Scenario-conditioned policy uncertainty

The lower layer introduces policy uncertainty conditioned on four regulatory scenarios: Conservative, Moderate, Optimistic, and Policy-Optimal. These scenarios represent impact of different levels of regulatory stringency on policy-sensitive cost components. CAPEX and maintenance costs are assumed to be

independent of regulatory stringency and are therefore not scenario conditioned. Similarly, fuel prices are not projected under policy uncertainty because historical analysis as shown in Figure 4 indicates only a weak relationship between fuel and carbon prices. From Figure 4, the correlation between MGO and EUA prices is weak (Pearson $r = 0.16$), while LNG prices exhibit virtually no correlation with EUA prices (Pearson $r = -0.01$). Hence, only policy-sensitive variables including EUA price, CO_2 value, FuelEU surplus credits, and IMO GFI surplus credits are adjusted in this layer.

Table 3 summarises the scenario-specific assumptions applied to the policy-sensitive parameters. For EUA prices, scenario-conditioned annual price paths are derived from the upper layer baseline using Equation 10:

$$P_t^{(s)} = P_{t,\mathrm{P50}}^{\mathrm{base}} \cdot \alpha_s(t) \cdot \exp\left(\sigma_s(t) z_t - \frac{1}{2}\sigma_s(t)^2\right) \tag{10}$$

where $P_{t,\mathrm{P50}}^{\mathrm{base}}$ is the median (P50) EUA price generated in the upper layer, α_s is a scenario-dependent scaling factor applied to the baseline trajectory, $\sigma_s(t)$ is a scenario-dependent uncertainty parameter controlling the dispersion of simulated prices, and the $z_t \sim \mathcal{N}(0,1)$ is a random number drawn from a standard normal distribution [50]. Under the Conservative scenario, the baseline EUA trajectory is adjusted downward through lower values of α_s and lower uncertainty range (σ_s). Moving from Conservative to Policy-Optimal scenarios, the EUA trajectory is progressively shifted upward through higher scaling factors (α_s), while larger values of σ are used to reflect the increasing uncertainty associated with long-term carbon-market evolution.

For the captured CO_2 value, scenario conditioning is implemented through regime selection (cost regime, market regime). As shown in Table 3, Conservative scenarios assume persistently high CO_2 offloading costs, while Optimistic scenarios assume lower offloading costs. In the Policy-Optimal scenario, a CO_2 market regime is activated, whereby captured CO_2 may be sold to generate revenue. Consequently, the captured CO_2 cost transitions from a disposal cost to a potential revenue stream within the techno-economic assessment.

For FuelEU Maritime and IMO GFI surplus-credit prices, Conservative scenarios emphasise lower surplus-credit values, while Optimistic and Policy-Optimal scenarios shift surplus credit towards higher surplus, with the Policy-Optimal assumed a surplus value approaching regulatory penalty levels (Cap regime), representing stronger incentives for low-carbon compliance.

Table 3. The lower layer scenario-conditioned policy parameters. The EUA scaling factor (α_s) adjusts the upper layer median EUA trajectory, while the uncertainty parameter (σ_s) controls the dispersion of simulated prices around the adjusted trajectory. The relative magnitudes shown (low to very high) represent increasing policy ambition and carbon-market stringency from Conservative to Policy-Optimal scenarios. The Captured CO_2, FuelEU Maritime surplus credits, and IMO GFI surplus credits are represented using regime-based assumptions reflecting alternative policy and market conditions.

Scenario	*EUA multiplier* $\alpha_s(t)$	*EUA uncertainty* $\sigma_s(t)$	*Captured* CO_2 *value*	*FuelEU surplus credit*	*GFI surplus credit*
Conservative	Low	Low	High-cost regime	Low regime	Low regime
Moderate	Moderate	Moderate	Moderate-cost regime	Moderate regime	Moderate regime
Optimistic	High	High	Low-cost regime	High regime	High regime
Policy-Optimal	Very high	Very high	CO_2 market regime	Cap regime	Cap regime

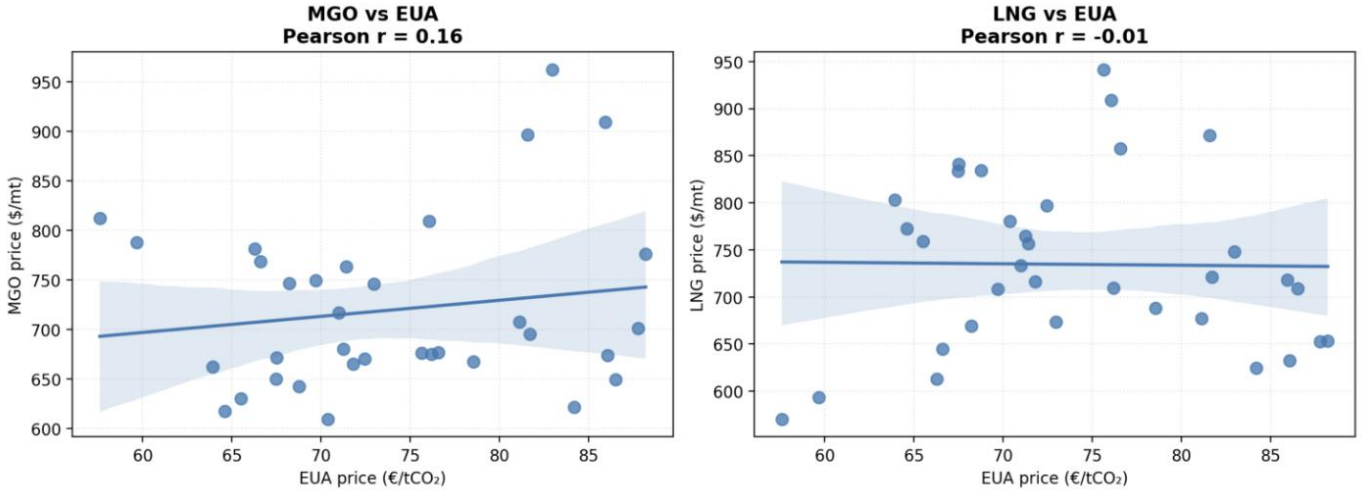


Figure 4. Historical relationship between fuel prices and EUA carbon prices based on monthly market data. The analysis indicates a weak positive correlation between MGO and EUA prices (Pearson r=0.16) and between LNG and EUA prices (Pearson r=−0.01). These results suggest that fuel-price dynamics are largely independent of carbon-price movements and therefore are modelled separately from policy-conditioned uncertainty scenarios.

In summary, the lower layer does not introduce new stochastic processes but modifies the distributions of policy-sensitive variables generated in upper layer to reflect each regulatory scenario. By integrating both models, policy-sensitive cost variables are represented as scenario-dependent probabilistic distributions, as illustrated in Figure 5. Clear scenario separation is observed for EUA prices, captured CO_2 prices, FuelEU surplus-credit prices, and IMO GFI surplus-credit prices. The Conservative scenario consistently produces the lowest EUA and surplus-credit values, reflecting weaker regulatory stringency and lower economic incentives for overcompliance. The scenario supports conventional propulsion with fossil fuels. In contrast, the Policy-Optimal scenario generates substantially higher surplus-credit valuations, indicating stronger regulatory support for low-carbon pathways. The FuelEU and GFI surplus-credit distributions exhibit comparatively wider spreads due to the bounded stochastic distributions and uncertainty associated with future credit-market behaviour and policy implementation.

The captured CO_2 value demonstrates the largest scenario differentiation, ranging from positive disposal costs under the Conservative scenario to negative values (–€50/ton CO_2) under the Policy-Optimal scenario. Negative CO_2 value represents market conditions in which captured carbon generates economic revenue through utilisation or market-based mechanisms. Overall, these policy-driven uncertainties directly propagate

into lifecycle cost calculations, influencing both the magnitude and variability of pathway competitiveness under long-term regulatory conditions.

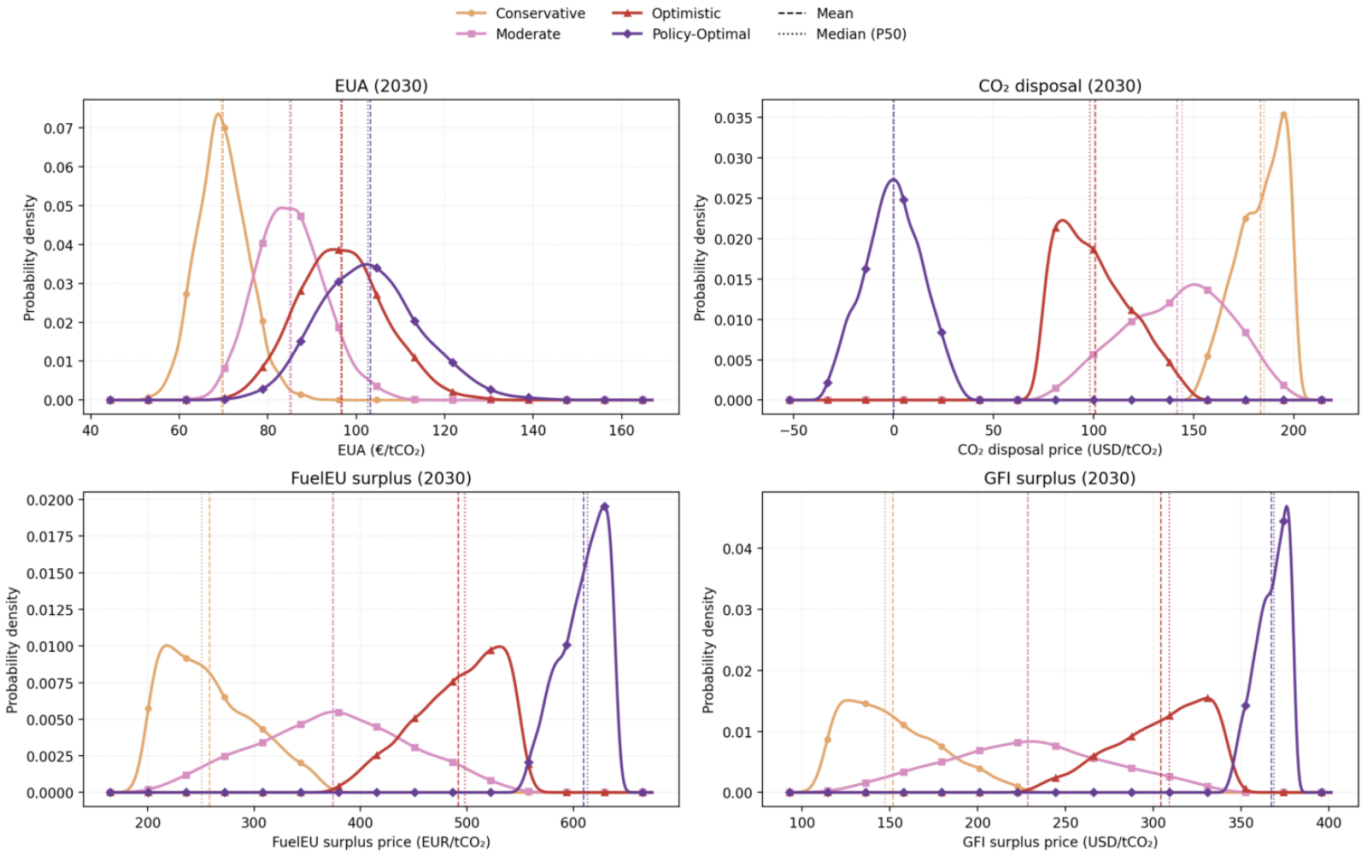


Figure 5. Probability density functions (PDFs) of annual policy variables in 2030 under different policy scenarios. Distributions are shown for EUA price, CO_2 value, FuelEU surplus credit, and GFI surplus credit, with mean and median indicators (Sample size of simulation, N = 3,500).

2.4.3 Layers integration and output metrics

The stochastic market and policy variables generated in the previous steps are integrated into the ship-level financial model (Equation 2) on an annual basis. For each Monte Carlo simulation *i*, year *t*, and policy scenario *s*, the corresponding fuel price, EUA price, CO_2 offloading cost, FuelEU surplus price, and GFI surplus price are passed into the financial model. The model subsequently recalculates all annual cost components and the cumulative lifecycle cost (Equation 3) for each simulation realisation and policy scenario. CAPEX uncertainty is also introduced which is randomly sampled within ±50% or ±15% of the baseline CAPEX depending on technology maturity. Consequently, the maintenance cost of the engine which is assumed equal to 2.5 – 4% of total CAPEX are also affected.

The annual total cost for each realisation is expressed as:

$$C_{\text{total}}^{i,t,s} = \int (X_{\text{CAPEX}}^{i}, X_{\text{fuel}}^{i,t}, X_{\text{EUA}}^{i,t,s}, X_{\text{CO}_2}^{i,t,s}, X_{\text{FuelEU}}^{i,t,s}, X_{\text{GFI}}^{i,t,s}) \tag{11}$$

which can be decomposed as:

$$C_{\text{total}}^{i,t,s} = C_{\text{CAPEX}}^{i} + C_{\text{fuel}}^{i,t} + C_{\text{m}}^{i,t} + C_{\text{CO}_2}^{i,t,s} + C_{\text{ETS}}^{i,t,s} + C_{\text{FuelEU}}^{i,t,s} + C_{\text{GFI}}^{i,t,s} \tag{12}$$

where i denotes the number of simulations, t denotes the year, and s denotes the policy scenario.

For each simulation, the cumulative lifecycle cost over the assessment period is obtained as:

$$C_{\text{cum}}^{i,s} = \sum_{t=t_0}^{t_1} C_{\text{total}}^{i,t,s} \tag{13}$$

The cumulative cost distributions are then evaluated using percentile-based indicators, including P10, P50, and P90, for both total lifecycle cost and individual cost components.

To check statistical convergence of the results, the sensitivity to the number of samples is quantified. As shown in Figure 6, the RefShip and HPU pathways exhibit comparatively more stable convergence behaviour than the Green H_2. The Green H_2 pathway only achieves relative absolute error below 1% for P10, P50, and P90 estimates at sample size of approximately N=3,500. Therefore, all stochastic variables are simulated over 3,500 realisations.

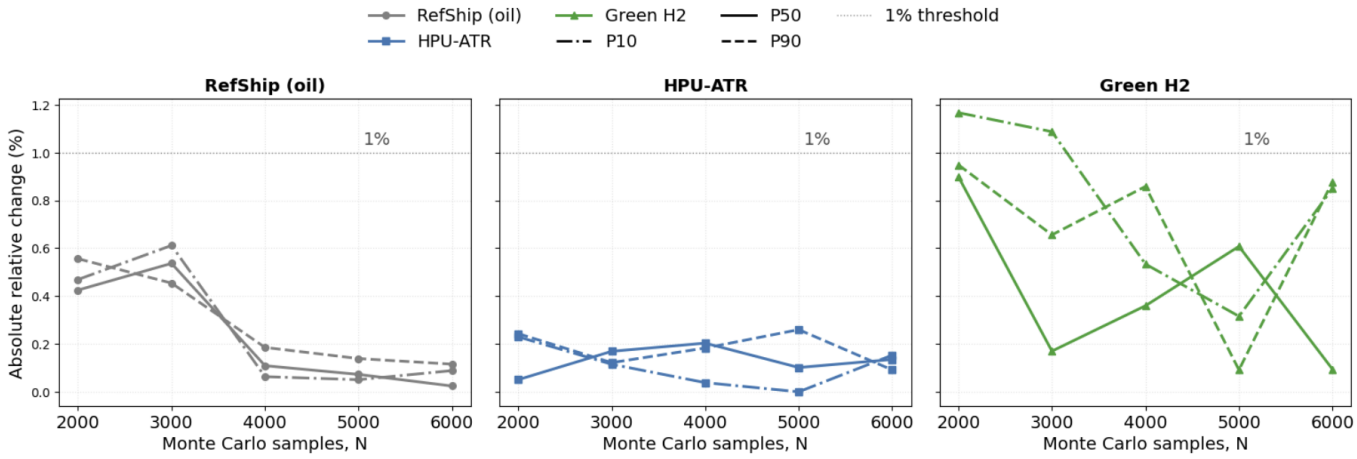


Figure 6. Monte Carlo convergence assessment based on percentile (P10/P50/P90) stability of cumulative lifecycle cost distributions. The dotted line indicates the 1% convergence threshold.

2.4.4 Comparison metrics

To compare the economic performance of each low-carbon pathway against the reference ship, a cumulative lifecycle cost ratio is defined as:

$$R^{(i,s)} = \frac{C_{\text{Case}}^{(i,s)}}{C_{\text{RefShip}}^{(i,s)}} \tag{14}$$

where $R < 1$ indicates that the low-carbon configuration is economically favourable as compared to the reference ship.

The probability that a pathway is cheaper than the reference ship is evaluated as:

$$P_{p,s} = \frac{1}{N}\sum_{i=1}^{N} I\left(C_{p,s}^{(i)} < C_{\text{RefShip},s}^{(i)} \right) \times 100 \tag{15}$$

where:

- N is the total number of Monte Carlo simulations,
- $I(\cdot)$ is an indicator function equal to 1 when the pathway cost is lower than the reference ship for the same Monte Carlo realisation, and 0 otherwise.

To analyse the performance when surplus-credit revenues are not available, an additional gross lifecycle cost metric is introduced. Unlike the net lifecycle cost, the gross lifecycle cost excludes FuelEU and IMO GFI surplus-credit revenues and therefore reflects the underlying physical and operational cost structure of each pathway.

The gross lifecycle cost is defined as (modified from Equation 2):

$$C_{\text{gross}} = C_{\text{fuel}} + C_{\text{CAPEX}} + C_{\text{maintenance}} + C_{\text{EUETS}} + C_{\text{FuelEU penalty}} + C_{\text{GFI penalty}} + C_{\text{CO2 offload}} \tag{16}$$

The corresponding gross lifecycle cost ratio is then expressed as:

$$R_{\text{gross}} = \frac{C_{\text{gross,Case}}}{C_{\text{gross,RefShip}}} \tag{17}$$

where:

- $R_{\text{gross}} < 1$indicates intrinsic techno-economic competitiveness relative to the reference ship,
- $R_{\text{gross}} > 1$indicates higher underlying cost before policy-credit revenues are considered.

Similarly, the probability of gross-cost competitiveness is evaluated as:

$$P_{\text{gross}} = \frac{1}{N}\sum_{i=1}^{N} I\left(C_{\text{gross,pathway}}^{(i)} < C_{\text{gross,RefShip}}^{(i)} \right) \times 100 \tag{18}$$

This formulation (Equation 15, Equation 18) enables separation between intrinsic techno-economic competitiveness and policy-enhanced competitiveness arising from surplus-credit mechanisms.

2.4.5 Threshold sensitivity analysis

By using the cumulative lifecycle cost ratio ($R^{(i,s)}$) obtained from Equation (14), a threshold analysis was performed to identify the market and policy conditions under which each pathway becomes cost-competitive with the reference vessel. For the $R^{(i,s)}$ obtained from each simulation realisation simulation i, year t, and policy scenario s, grouping is carried out according to the realised value of a single stochastic cost parameter (also referred to as driver) of interest, including EUA price, FuelEU surplus price, GFI surplus price, green hydrogen price and CO_2 offloading cost ($X_{EUA}^{i,t,s}$, $X_{FuelEU}^{i,t,s}$, $X_{GFI}^{i,t,s}$, $X_{H2\,fuel}^{i,t,s}$, $X_{CO_2}^{i,t,s}$).

The time-averaged realised value of that selected drivers over the evaluation window (2030 – 2050) is computed for each simulation realisation and then grouped into quantile bins according to this averaged value. Within each bin, the median (P50) and 10th–90th percentile band (P10–P90) are evaluated. As the $R^{(i,s)}$ is computed from realisations in which all stochastic cost parameters vary jointly, grouping by one driver does not fix the others: each bin retains the values the remaining cost parameters took in their respective joint realisation. The resulting P10–P90 band therefore reflects both the sensitivity of $R^{(i,s)}$ to the binned driver and the residual variability contributed by the co-varying cost parameters within that bin.

The value of the binned driver at which the median curve crosses unity ($R = 1$ or RefShip = 1) indicates the approximate threshold at which the pathway becomes cost-competitive with the reference vessel on a median basis, consistent with the competitiveness criterion $R < 1$ established in Equation (14).

3. RESULTS AND DISCUSSION

3.1. Deterministic baseline results (reference case)

Figure 7 shows the key cost breakdown of the reference ship over the 2030 – 2050 assessment period using representative deterministic values for all cost components (calibrated X_{eq} of MGO: \$892/t, calibrated X_{eq} of LNG: \$772/t, X_{mode} of Green H_2: \$5/kg, CO_2 offloading: \$125/tCO_2, EUA: €150/tCO_2, X_{min} for both FuelEU and IMO GFI surplus credit: credited at 30% of the penalty price for instance, \$191.7/ton FuelEU surplus and \$114/ton GFI surplus). For reference ship (RefShip), the total annual net cost (C_{total}) is projected to increase significantly from ~\$26 million to ~\$60 million in 2050, when emission penalties (EUA, FuelEU and GFI) were included. The CAPEX and maintenance contribute only a minor share of the total lifecycle cost compared to fuel and regulatory penalties. Overall, policy-related penalties contribute more than 50% of the cumulative lifecycle cost over the assessment period, corresponding to ~\$445 million. The remaining

cost is primarily attributed to fuel expenditure (~$365 million) and engine-related CAPEX and maintenance (~$26 million).

In contrast, hydrogen-based propulsion pathways substantially reduce emissions-related penalties. As shown in Figure 8, the results demonstrate a strong divergence in cost structure between the two hydrogen supply pathways under the Conservative scenario.

For the HPU pathway (Figure 8(a)), the cost structure remains relatively diversified. Although fuel remains a major contributor, substantial cost contributions also arise from CO_2 offloading, CAPEX, maintenance, and policy-related costs including EU ETS and FuelEU penalties. This reflects the presence of residual emissions associated with upstream (well-to-tank) emissions and incomplete carbon capture, which continue to expose the pathway to carbon-pricing mechanisms. Carbon-related costs contribute approximately 26% of C_{total}, including 18.6% for captured CO_2 offloading. Consequently, the HPU pathway exhibits multi-dimensional cost exposure, particularly to policy stringency and carbon management economics. Nevertheless, the pathway is also capable of generating surplus credits under FuelEU Maritime and IMO GFI through overcompliance with emissions targets.

In contrast, the Green H_2 pathway (Figure 8(b)) exhibits a significantly more fuel-dominated cost structure of fuel cost over the long-term assessment horizon. Fuel expenditure accounts for approximately 85% of total gross lifecycle cost (~$730 million out of ~$850 million), while CAPEX, maintenance, and policy-related costs contribute only marginally. As a zero tank-to-wake (TTW) emission pathway, Green H_2 incurs minimal emissions penalties and eliminates the need for onboard CO_2 capture and offloading. This effectively decouples the pathway from carbon-pricing exposure. However, the economic performance of Green H_2 becomes highly dependent on hydrogen fuel price, which is assumed at $5/kg in this study. These results highlight the importance of hydrogen price reduction and fuel-market sensitivity analysis for large-scale adoption of green-fuel propulsion systems.

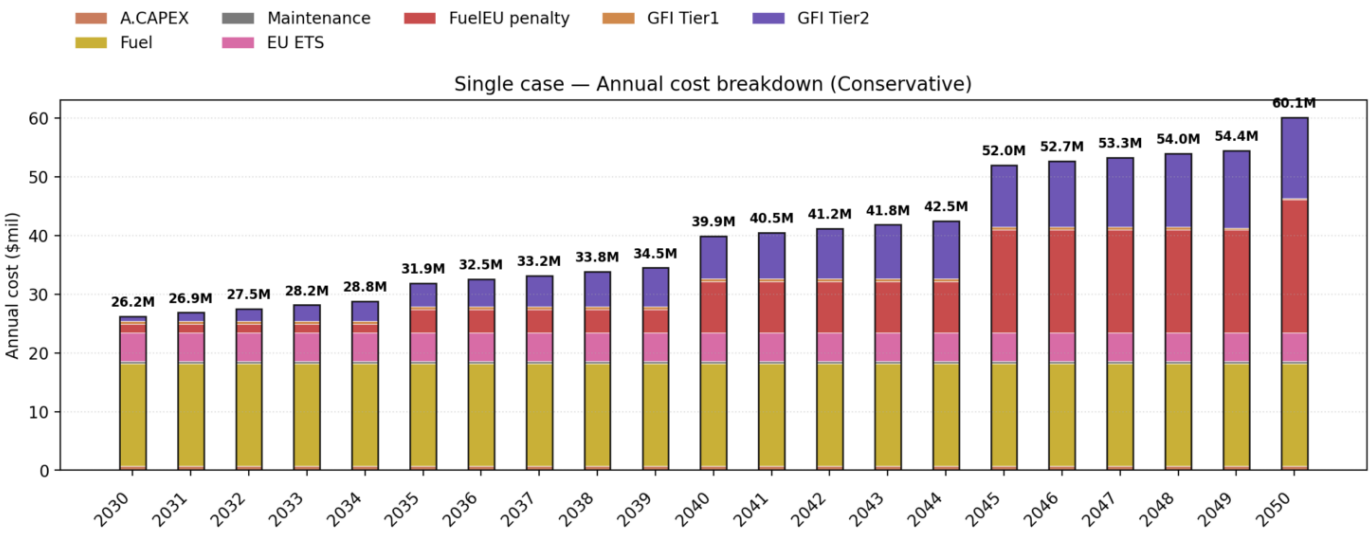
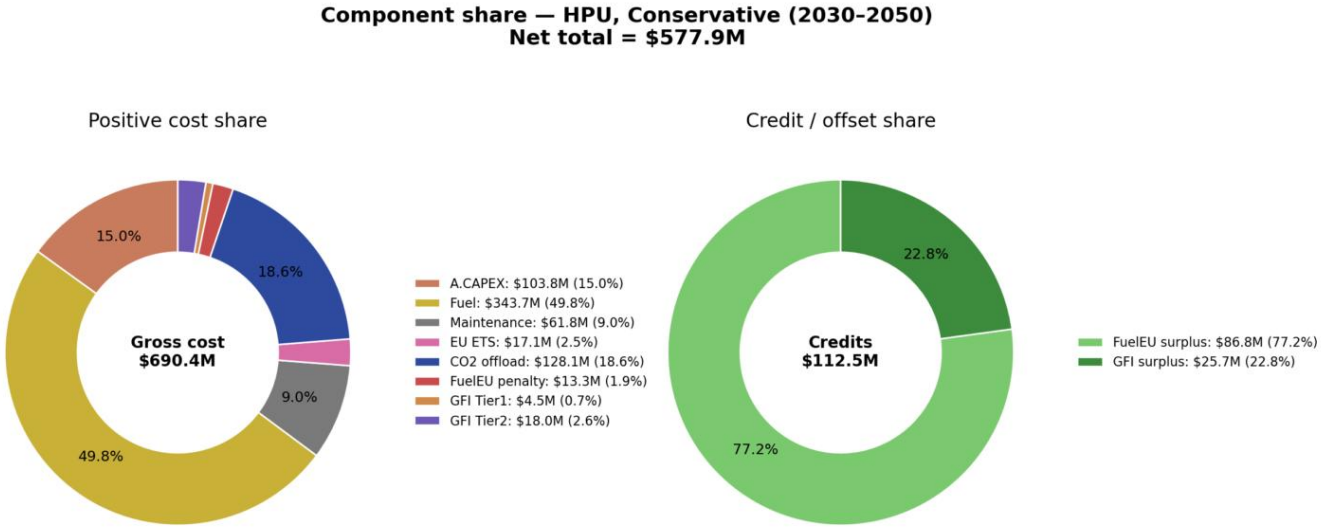
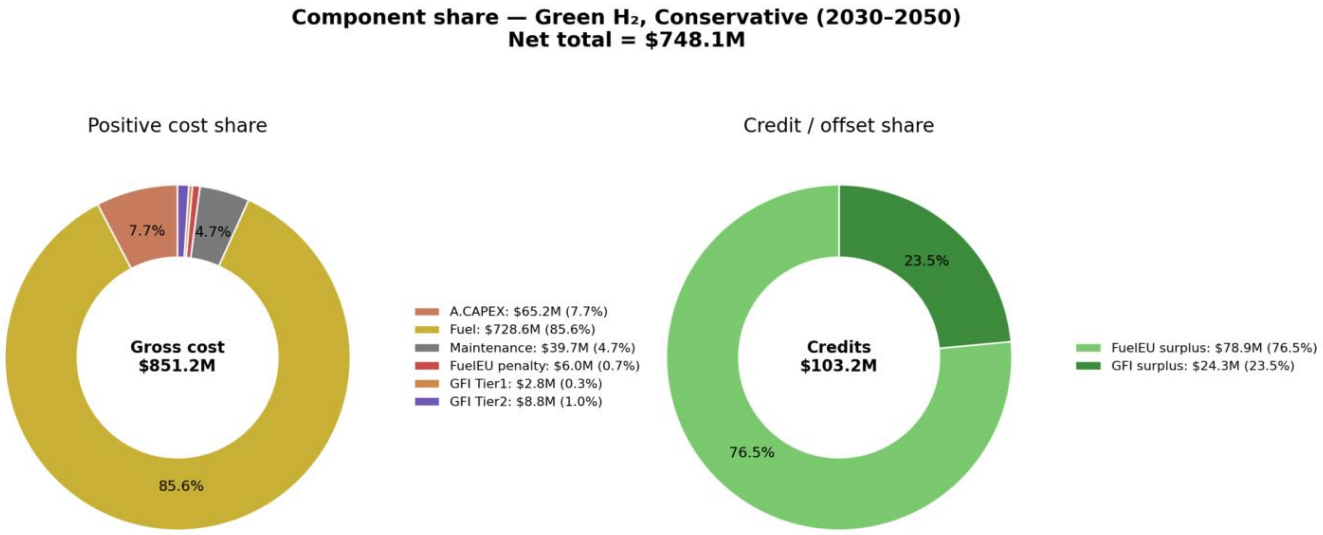


Figure 7. Deterministic projection of the total annual lifecycle cost (C_{total}) for reference ship fuelled with MGO (RefShip) between 2030-2050.



(a)



(b)

Figure 8. Deterministic projection of the cumulative cost (2030–2050) for all cost component under the conservative policy scenario for two hydrogen pathways. (a) Onboard hydrogen production via HPU system, and (b) Green hydrogen supply case, where the hydrogen price is assumed to be $5/kg. Surplus-credit revenues under FuelEU Maritime and IMO GFI are estimated based on conservative assumptions with CO_2 surplus credited at 30% of the penalty price.

Next, Figure 9 presents the cumulative lifecycle cost breakdown for all propulsion pathways under four deterministic policy scenarios. Each scenario assumes a different level of regulatory support through variations in surplus-credit valuation. The surplus credits for FuelEU and IMO GFI are valued at 30%, 60%, 90% and 100% of the corresponding penalty price under the Conservative, Moderate, Optimistic, and Policy-Optimal scenarios, respectively. For all deterministic scenarios, the EUA price and CO_2 offloading value are held constant at €150/tCO_2 and $125/t$CO_2$, respectively.

As shown in Figure 9 , as the surplus-credit valuation increases from Conservative to Policy-Optimal scenarios, the economic benefit obtained from FuelEU Maritime and IMO GFI overcompliance also increases substantially. Consequently, the net cumulative lifecycle cost of the hydrogen pathways decreases progressively under more supportive regulatory conditions, improving their relative competitiveness against the conventional reference ship. These results indicate that policy design can significantly reshape the economic attractiveness of maritime decarbonisation pathways by shifting lifecycle cost structures from fuel-dominated expenditure toward regulatory and incentive-driven mechanisms.

The analysis presented in Figure 9 is based on deterministic policy assumptions with predefined surplus-credit values. In practice, both market variables (e.g., fuel prices) and policy-related parameters (e.g., carbon prices and surplus-credit valuation) are subject to market and policy fluctuations. To capture the interaction between market and regulatory uncertainty, the following section introduces the results from the Monte Carlo framework for probabilistic lifecycle cost assessment.

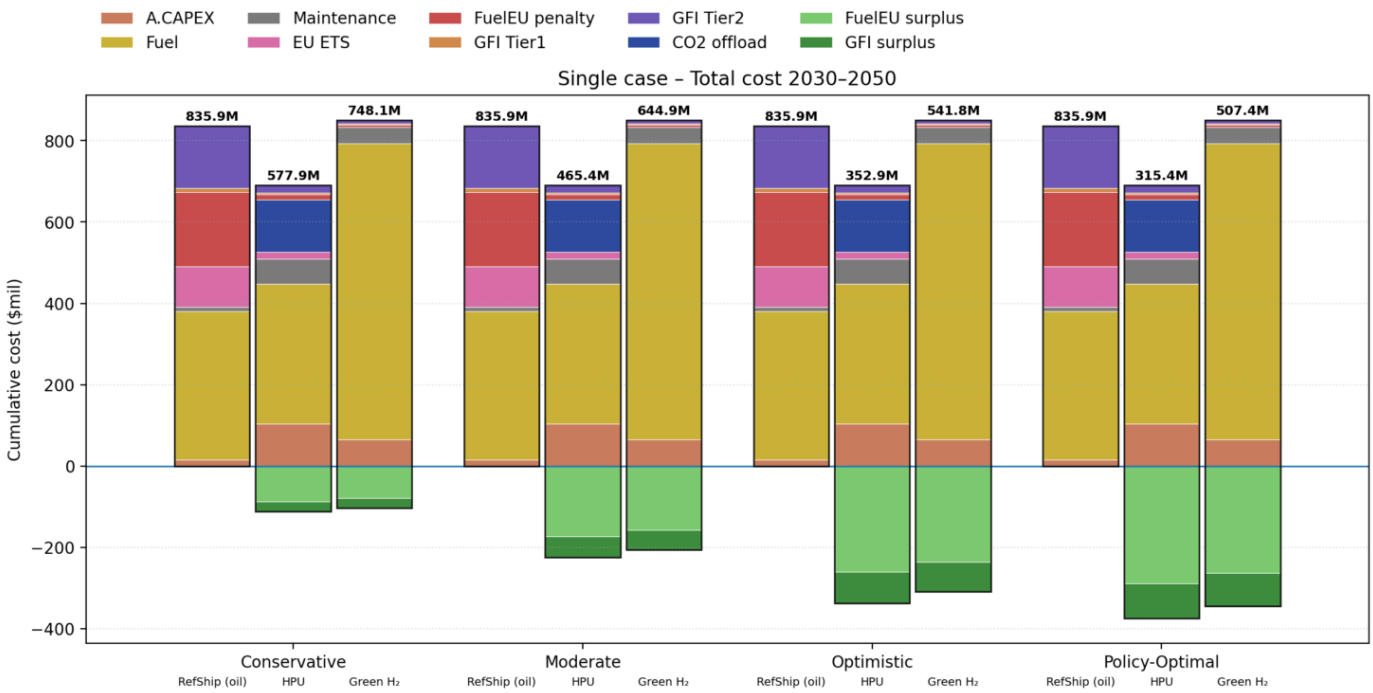


Figure 9. Deterministic projection of the cumulative lifecycle cost breakdown (2030–2050) for the reference ship (RefShip), onboard hydrogen production (HPU), and green hydrogen (Green H_2) pathways under different policy scenarios (conservative, moderate, optimistic, and policy-Optimal). Surplus-credit values are assumed to be 30%, 60%, 90%, and 100% of the corresponding penalty value, respectively. Costs are disaggregated into major components including CAPEX, fuel, maintenance, EU ETS, CO_2 offloading, FuelEU penalties, and GFI contributions, while negative values represent policy-driven credits (FuelEU and GFI surplus). EUA price and CO_2 offloading value are fixed at €150/tCO_2 and $125/t$CO_2$ across all scenarios.

3.2. Monte Carlo results: lifecycle cost uncertainty

This section presents the probabilistic lifecycle cost assessment obtained using the Monte Carlo framework. The analysis first examines uncertainty propagation across individual lifecycle cost components, followed by probabilistic assessment of total lifecycle cost and pathway competitiveness.

3.2.1 Cost component uncertainty analysis

Figure 10 presents the decomposition of cumulative lifecycle cost into key components for each propulsion pathway, including uncertainty ranges derived from Monte Carlo simulations (P10–P90). For the conventional RefShip pathway, fuel cost and emission penalties both are the dominant contributors. The fuel cost exhibits relatively narrow uncertainty bands, reflecting the comparatively stable fuel price behaviour calibrated from historical market data. Policy penalties including FuelEU Maritime and IMO GFI are primarily governed by regulatory penalties, leaving EUA price as the main policy-sensitive contributor.

In contrast, the HPU exhibits a more distributed cost structure, with notable contributions from LNG fuel cost, CO_2 offloading, and policy-related components, alongside substantial negative contributions from

FuelEU Maritime and IMO GFI surplus credits. The comparatively wider uncertainty ranges associated with these components indicate stronger sensitivity to both market and policy conditions.

The green H_2 configuration is strongly dominated by fuel expenditure, which contributes the majority of the total lifecycle cost. Due to the possibility of technology improvement, there is wider uncertainty bands for fuel price. Hence, hydrogen price uncertainty is the primary driver of overall lifecycle cost variability. Policy-related costs play a comparatively secondary role, mainly affecting lifecycle cost through surplus-credit mechanisms.

Overall, the results demonstrate that fuel-price uncertainty dominates lifecycle cost variability across all pathways, while policy-sensitive components introduce additional uncertainty and potential cost reduction opportunities for low-carbon configurations.

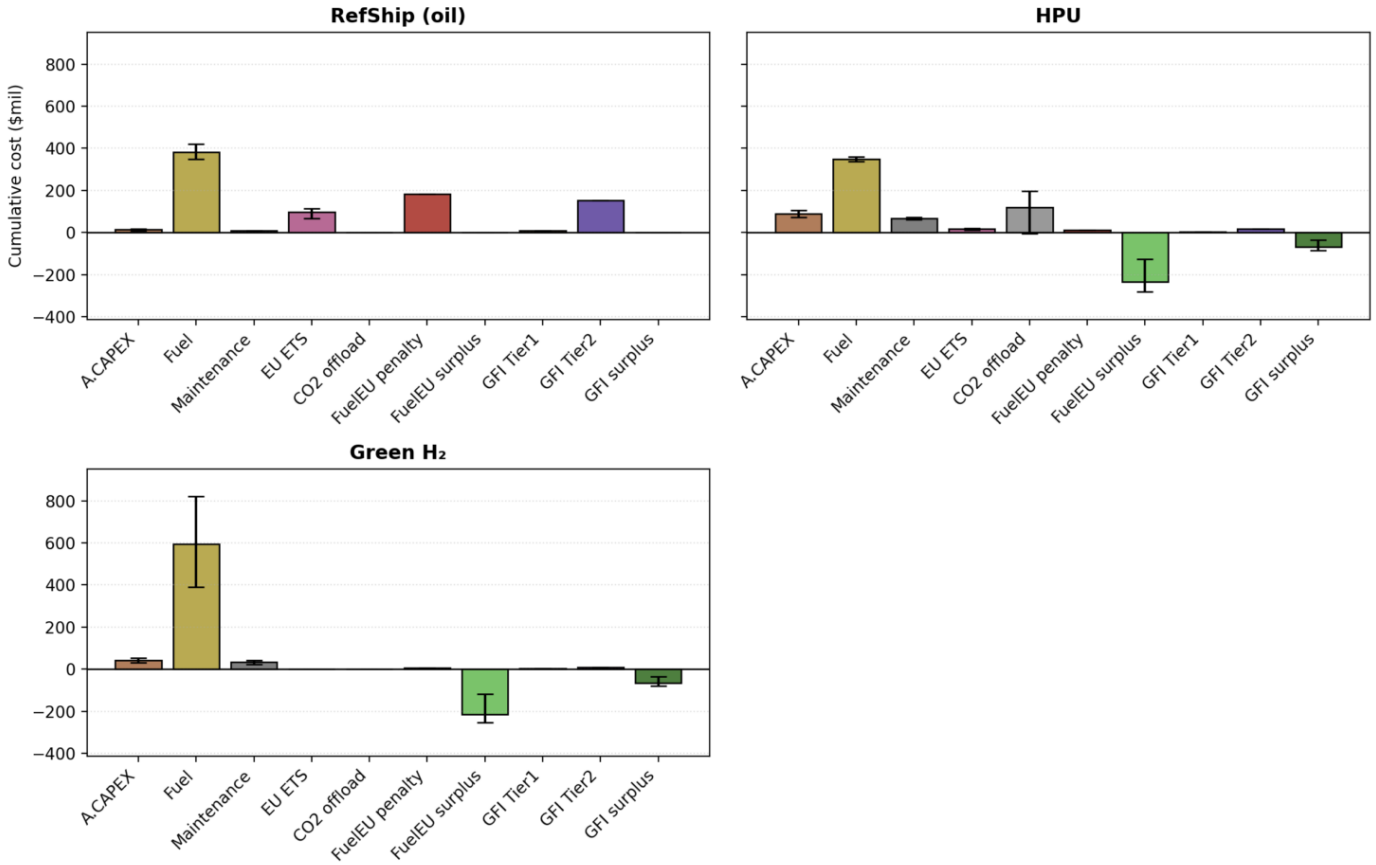


Figure 10. Decomposition of cumulative lifecycle cost by component with uncertainty ranges (P10–P90) over the 2030–2050 assessment period. Bars represent the median (P50) cumulative cost contribution of each component, while error bars indicate the P10–P90 uncertainty range obtained from Monte Carlo simulations (N=3,500) under all policy scenarios, illustrating the variability of key lifecycle cost contributors across alternative propulsion pathways.

3.2.2 Probability distribution of cumulative lifecycle cost ($C_{total,cum}$)

The propagation of uncertainty from both market dynamics and policy variables into total net lifecycle cost ($C_{total,net}$) is assessed in Figure 11. The figure presents the probability density distributions of cumulative lifecycle cost over the 2030–2050 period for different propulsion pathways under four policy scenarios.

Among all configurations, the probability density of the RefShip is narrower and centres at higher cumulative lifecycle cost region across most policy scenarios, indicating comparatively stable economic performance at high cumulative cost. The HPU has wider PDFs, but shifted to lower cumulative costs, mostly due to the benefits associated with monetising carbon surpluses. Green H_2 exhibits the broadest uncertainty spread across all policy scenarios. This is primarily because the lifecycle cost is dominated by hydrogen fuel expenditure, while policy-related mechanisms act mainly as secondary modifiers through surplus-credit revenues. Consequently, the assumed future hydrogen price between \$2-\$8/kgH_2 drives the total cumulative lifecycle cost distribution over a wide range. As a result, the economic competitiveness of *G*reen H_2 remains strongly dependent on future reductions in hydrogen production, transportation, and bunkering cost.

Under the Policy-Optimal scenario, where captured CO_2 is assumed to possess positive market value and where green hydrogen is assumed to be cost competitive at ~\$2kg/H_2, the cumulative lifecycle cost for the hydrogen pathways decreases substantially, reaching median values as low as ~\$200 - \$400 million over the 20-year assessment period. This result indicates that low-carbon pathways may achieve strong economic competitiveness under favourable fuel-pricing and carbon-utilisation conditions. However, the long-term monetisation of captured CO_2 remains subject to regulatory acceptance and verification requirements associated with permanent carbon removal. The long-term alternative fuel prices are driven by the availability of renewable electricity and continued technology advancement.

Overall, the probabilistic results demonstrate that policy uncertainty plays a critical role in shaping decarbonisation competitiveness, while different propulsion pathways exhibit fundamentally different uncertainty and risk profiles. The results further highlight the importance of probabilistic modelling, given that a deterministic scenario analysis alone cannot adequately capture the full range of possible lifecycle cost outcomes and investment risks.

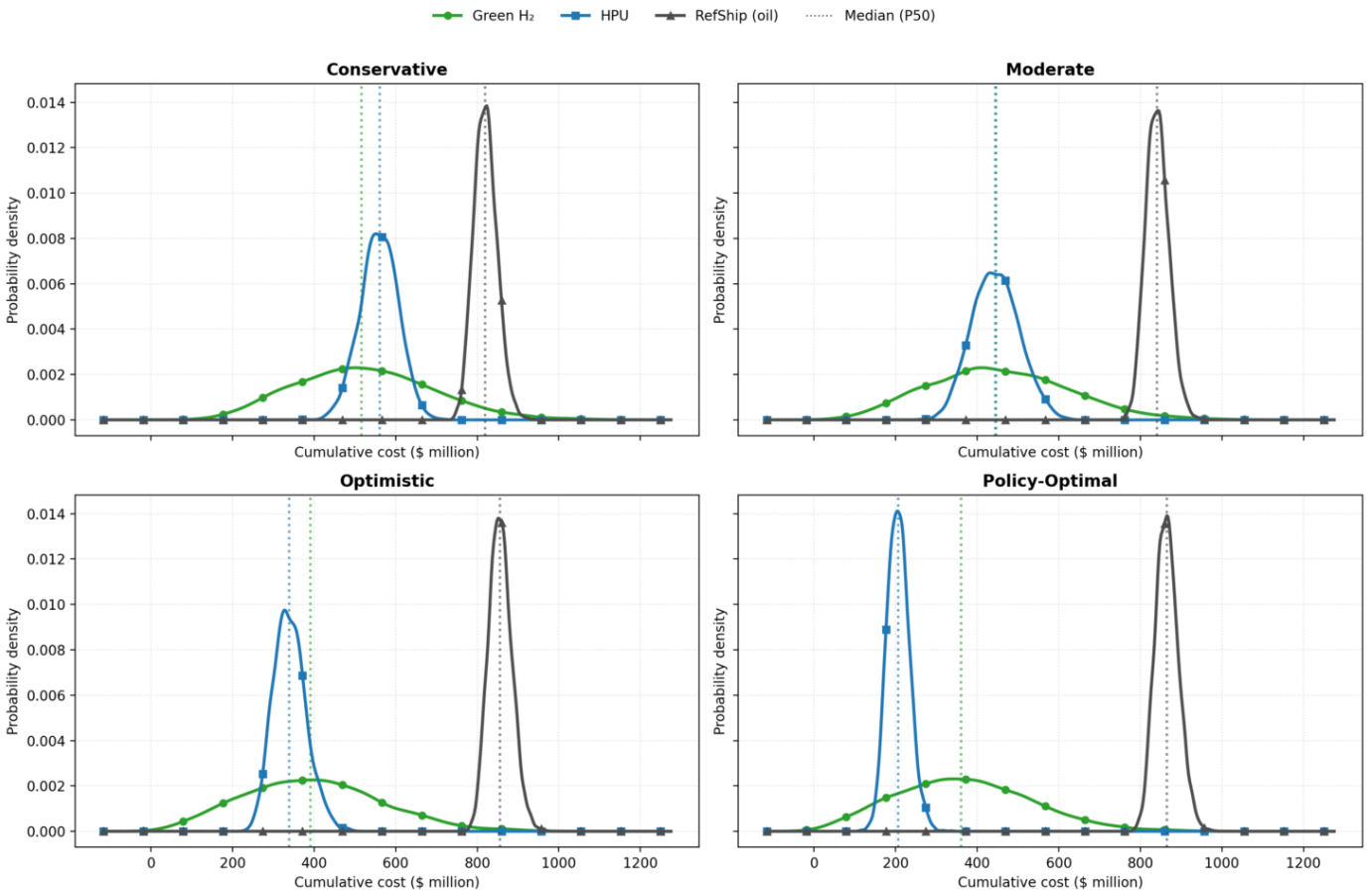


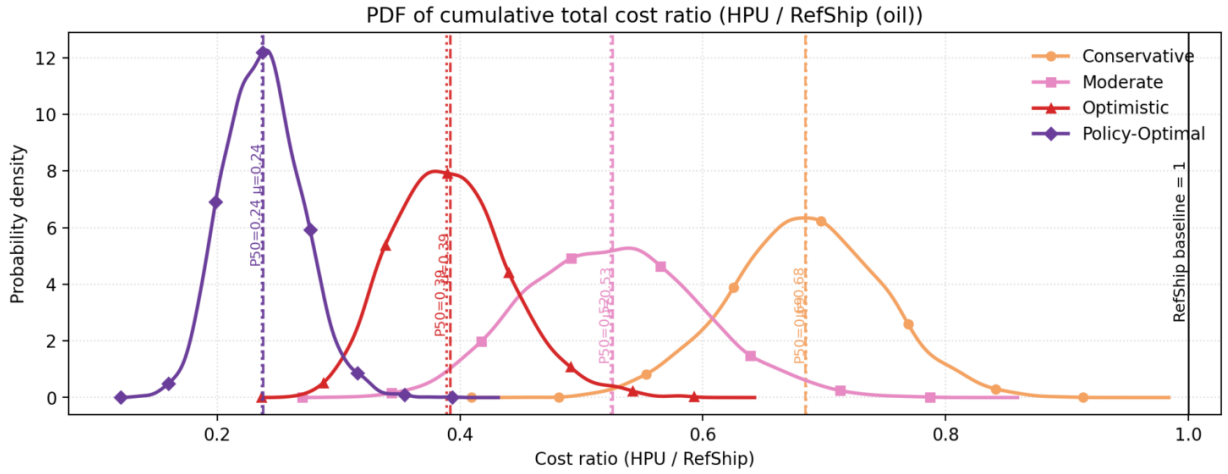
Figure 11. Probability density distributions of cumulative lifecycle cost (2030–2050) across policy scenarios and propulsion pathways with vertical dashed lines indicate the median cumulative cost (P50). Results are obtained using the Monte Carlo framework, capturing combined uncertainty from stochastic market dynamics (Upper layer) and scenario-conditioned policy uncertainty (Lower layer). Each subplot represents a policy scenario, illustrating the propagation of uncertainty into lifecycle cost variability.

Figure 12 presents the probability density distribution of the cumulative lifecycle cost ratio relative to the RefShip baseline under different policy scenarios, when both the hydrogen pathway and the reference ship are evaluated using the same realisation of stochastic fuel prices and policy-sensitive variables. In both hydrogen pathways, the distributions remain below the competitiveness threshold ($R = 1$), indicating that both hydrogen pathways are economically favourable relative to the conventional reference ship across most Monte Carlo realisations.

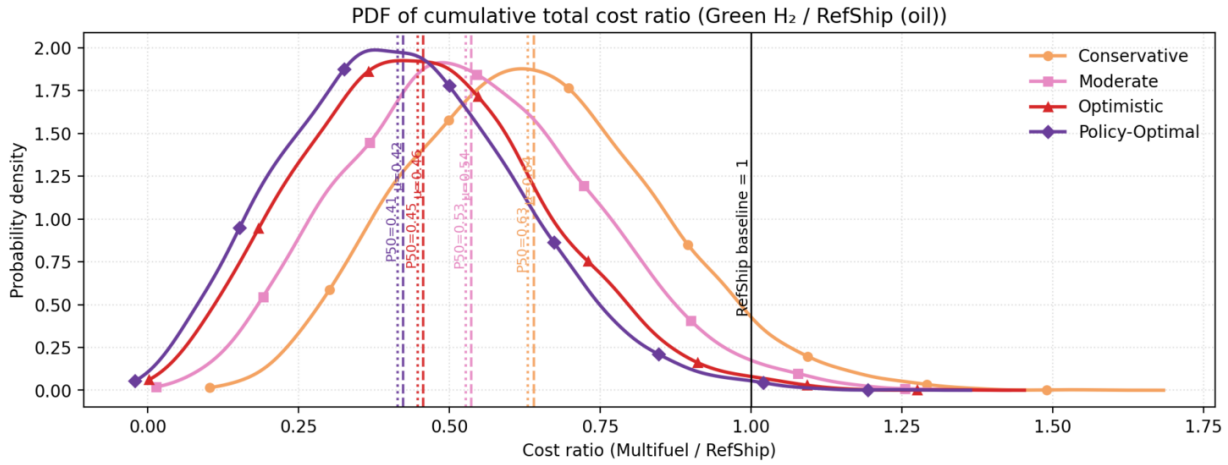
The HPU cost ratio distributions shift substantially leftward with increasing policy ambition from median value (P50) of 0.68 for Conservative scenario to 0.24 for Policy-Optimal scenario, indicating strong sensitivity to carbon pricing and surplus-credit mechanisms. The component breakdown in Figure 13 shows that this reduction is driven primarily by the growing magnitude of FuelEU and GFI surplus credits under Policy-Optimal scenarios, which offset a large share of HPU's gross cost and reduce its net median lifecycle cost to $202.0M, compared with $864.3M for RefShip. The reduction in lifecycle cost ratio under more

supportive policy scenarios demonstrates the strong influence of regulatory incentives and carbon-management economics on the competitiveness of OCCS pathways.

In contrast, the Green H_2 pathway demonstrates a comparatively weaker response to policy strengthening. Although the distributions also shift leftward with increasing policy ambition, the reduction in median lifecycle cost ratio is comparatively smaller, decreasing from approximately $R = 0.63$ under the Conservative scenario to approximately $R = 0.42$ under the Policy-Optimal scenario. The probability distributions also remain relatively broad, indicating continued sensitivity to hydrogen fuel-price uncertainty.



(a)



(b)

Figure 12. Probability density distributions of cumulative lifecycle cost ratios relative to the RefShip baseline for (a) HPU and (b) Green H_2 pathways under different policy scenarios over the 2030–2050 period. Vertical dashed lines indicate the median lifecycle cost ratio (P50) for each scenario, while the solid black line at R=1 represents cost parity with the conventional reference ship. Values below R=1 indicate economic competitiveness relative to the RefShip baseline.

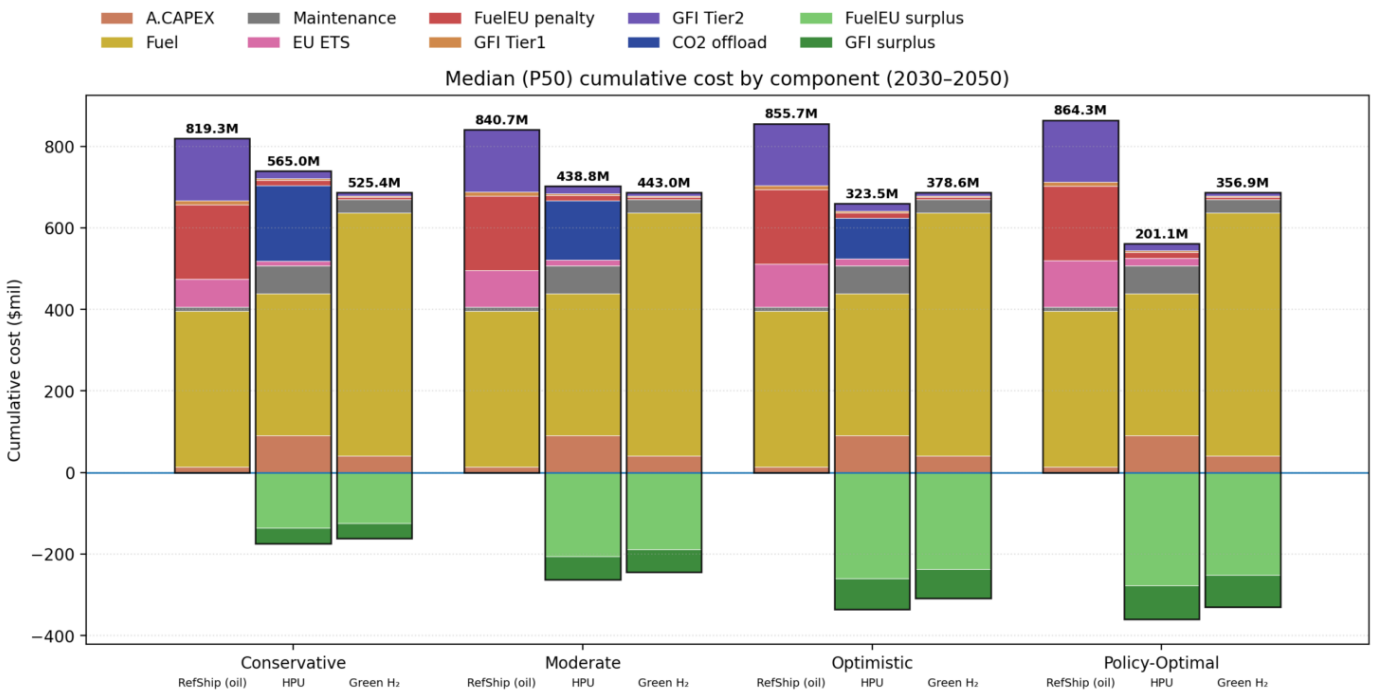


Figure 13. Median (P50) cumulative cost breakdown by component for the RefShip, HPU, and Green H_2 pathways under different policy scenarios (conservative, moderate, optimistic, and policy-Optimal) over the 2030–2050 period. Costs are disaggregated into major components including CAPEX, fuel, maintenance, EU ETS, CO_2 offloading, FuelEU penalties, and GFI contributions, while negative values represent policy-driven credits (FuelEU and GFI surplus).

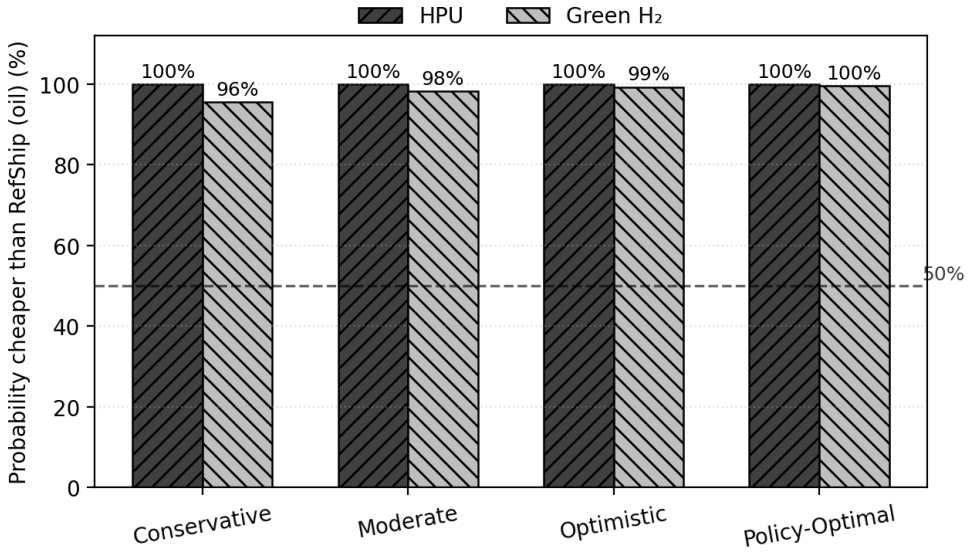
3.3. Risk-based cost competitiveness comparison

Figure 14 presents the probability that the alternative pathways achieve lower cumulative lifecycle cost than the RefShip baseline over the 2030–2050 assessment period under different policy scenarios. The results in Figure 14(a) indicate that when surplus-credit revenues are included, both hydrogen pathways demonstrate strong economic competitiveness relative to the conventional reference ship, with >96% probability to result in a lower lifecycle cost than RefShip. Between both pathways, HPU consistently exhibits a slightly higher probability of achieving lower lifecycle cost than Green H_2 across all policy scenarios.

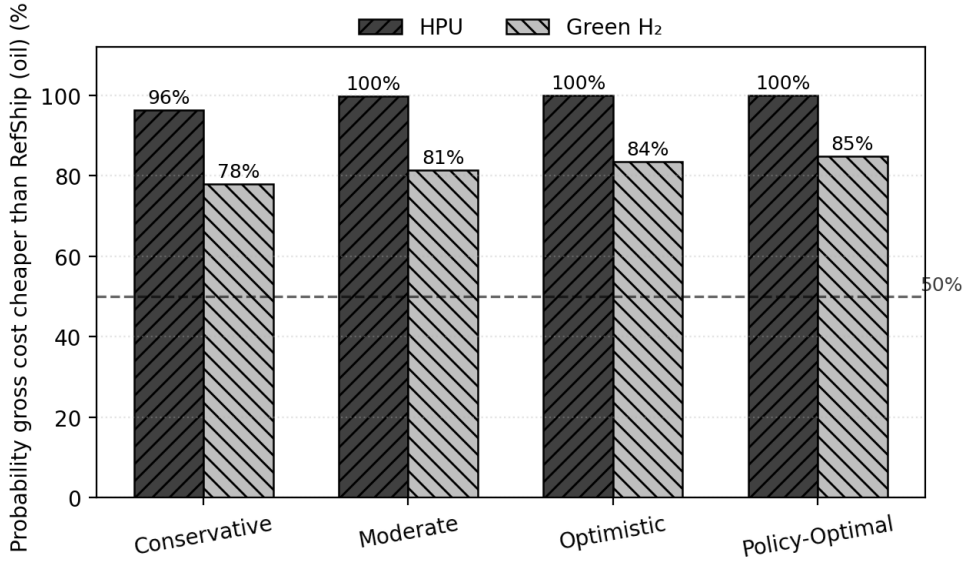
However, exclusion of FuelEU Maritime and IMO GFI surplus-credit revenues substantially reduces the competitiveness probability of both pathways. As shown in Figure 14(b), HPU maintains a comparatively high probability of lower gross lifecycle cost across all policy scenarios, increasing from 96% under the Conservative scenario to 100% under the Policy-Optimal scenario. This indicates that the onboard hydrogen production pathway remains economically favourable even without direct monetisation of surplus credits, reflecting relatively strong intrinsic competitiveness arising from lower emissions exposure.

In contrast, Green H_2 exhibits gross competitiveness probabilities between 78 to 85% across all scenarios, indicating an approximately 20% probability that the pathway would become more expensive than RefShip

once surplus-credit revenues are excluded. Although the pathway achieves near-zero Tank-to-Wake emissions, its competitiveness remains constrained by the uncertain cost of green hydrogen supply.



(a)



(b)

Figure 14. Risk-based cost competitiveness of HPU and Green H_2 pathways relative to the RefShip baseline over the 2030–2050 assessment period under different policy scenarios: (a) net lifecycle cost competitiveness including surplus-credit revenues, and (b) gross lifecycle cost competitiveness excluding FuelEU Maritime and IMO GFI surplus-credit revenues.

Figure 15 and Figure 16 present the gross lifecycle cost ratio of the alternative pathways relative to RefShip, excluding FuelEU Maritime and IMO GFI surplus-credit revenues.

As shown in Figure 15 and Figure 16 (a), the median gross lifecycle cost ratio for the HPU pathway decreases from approximately 0.90 under Conservative scenario to approximately 0.65 under the Policy-

Optimal scenario. This indicates that the HPU which scored a progressively lower gross cost ratio becomes more economically attractive relative to the RefShip under increasingly supportive regulatory conditions. While a small probability remains that HPU could be more expensive than the RefShip under the Conservative and Moderate scenarios (As shown in Figure 16 (a)), this probability becomes negligible under the Optimistic and Policy-Optimal scenarios. Furthermore, the uncertainty range narrows under more supportive policy scenarios, suggesting improved robustness of economic performance.

In contrast, Figure 15 and Figure 16 (b) show that the Green H_2 configuration maintains median gross lifecycle cost ratios at round R=0.8 across all policy scenarios. Although stronger policy support slightly reduces the gross cost ratio, the improvement remains modest because lifecycle costs are dominated by hydrogen fuel expenditure. The distribution under all scenarios continues to extend beyond R = 1, indicating a non-negligible probability that the Green H_2 pathway may remain more expensive than the RefShip. The policy strengthening reduces the gross cost ratio marginally, the improvement remains limited due to the dominant contribution of hydrogen fuel expenditure. The broader distribution of gross cost ratio further highlights the persistent sensitivity of the Green H_2 pathway to long-term hydrogen price uncertainty.

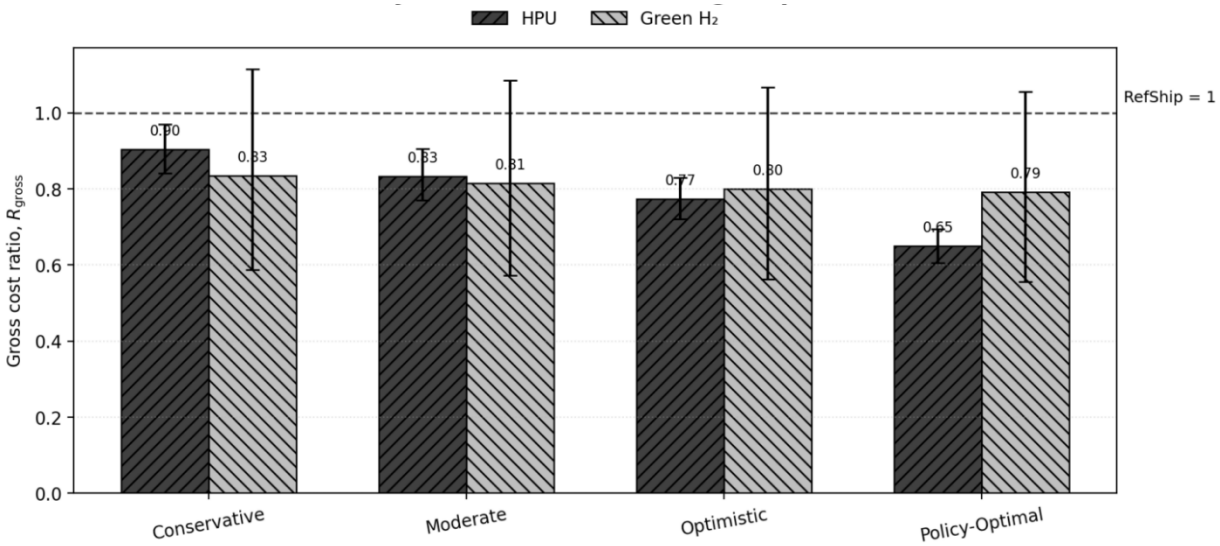
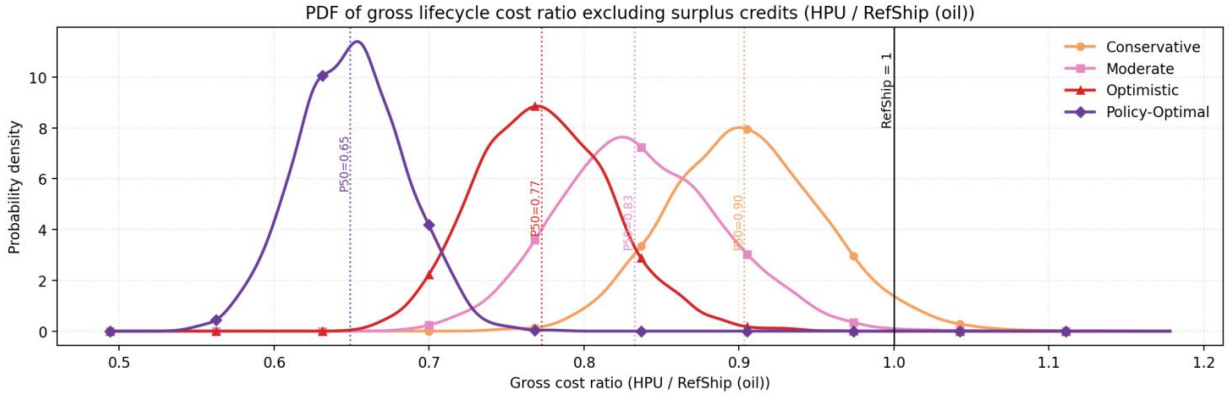
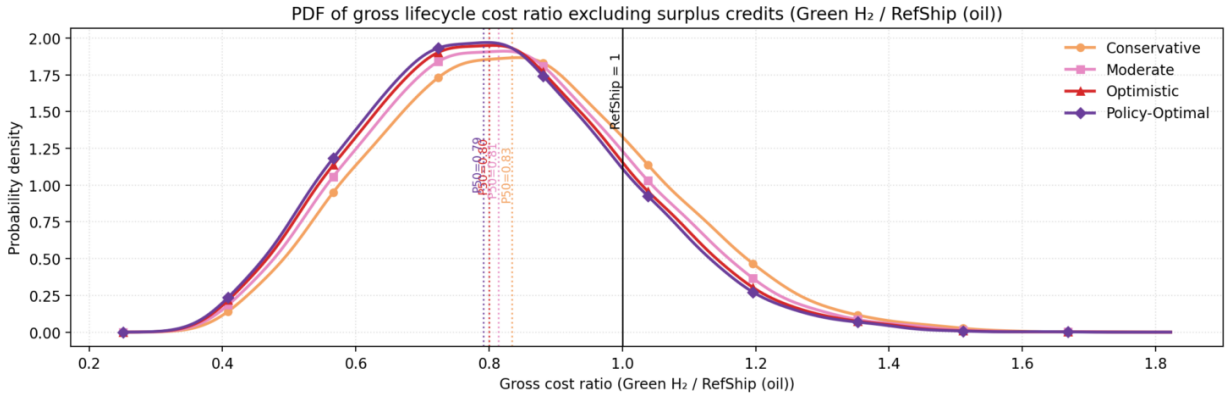


Figure 15. Gross lifecycle cost ratio of HPU and Green H_2 relative to RefShip, excluding FuelEU Maritime and IMO GFI surplus-credit revenues. Bars represent the median gross lifecycle cost ratio (P50), while error bars indicate the P10–P90 uncertainty range obtained from Monte Carlo simulations. Values below unity indicate lower gross lifecycle cost than the RefShip baseline.



(a)



(b)

Figure 16. Probability density distributions of cumulative gross lifecycle cost ratios relative to the RefShip baseline for (a) HPU and (b) Green H_2 pathways under different policy scenarios over the 2030–2050 period, excluding FuelEU Maritime and IMO GFI surplus-credit revenues. Vertical dashed lines indicate the median lifecycle cost ratio (P50) for each scenario, while the solid black line at R=1 represents cost parity with the conventional reference ship. Values below R=1 indicate economic competitiveness relative to the RefShip baseline.

Next, the threshold sensitivity analysis further highlights the different competitiveness drivers governing the two hydrogen pathways. Both pathways remain economically favourable relative to RefShip even under comparatively low EUA prices (~100 €/tCO_2), while competitiveness improves rapidly under increasingly stringent carbon-pricing conditions. Similarly, both hydrogen pathways maintain lifecycle cost ratios below unity even under relatively conservative (low) FuelEU Maritime and IMO GFI surplus-credit assumptions, indicating comparatively strong resilience even under a relatively weak policy-support conditions, as shown in Figure 17 (b)-(c).

Comparatively, Green H_2 shows higher lifecycle cost uncertainty, reflected by the wider green shaded P10/P90 band and P90 ranges approaching the unity threshold, as shown in Figure 17 (a)-(c). In contrast, HPU demonstrates a steeper median trend with relatively narrower uncertainty bands, indicating the more stable economic performance of HPU while remaining more responsive to carbon-pricing and surplus-credit mechanisms.

The competitiveness of Green H_2 is primarily constrained by hydrogen fuel cost (Figure 17(d)). The pathway remains economically favourable relative to RefShip only when hydrogen price remains below ~\$5.8/kg H_2. This suggests that large-scale deployment of Green H_2 propulsion is strongly dependent on substantial reductions in hydrogen production, transportation, and bunkering cost, together with continued support from emissions penalty and surplus-credit mechanisms.

In contrast, HPU demonstrates substantially stronger intrinsic economic performance across the investigated policy ranges. Although increasing CO_2 offloading cost gradually weakens HPU competitiveness (Figure 17 (e)), the pathway remains economically favourable across a broad range of CO_2 handling costs, suggesting relatively robust economic resilience of CCS-integrated propulsion systems under future carbon-management requirements. Extrapolation of the median trend further suggests that HPU may approach cost parity with RefShip when CO_2 offloading costs exceed ~\$300/tCO_2.

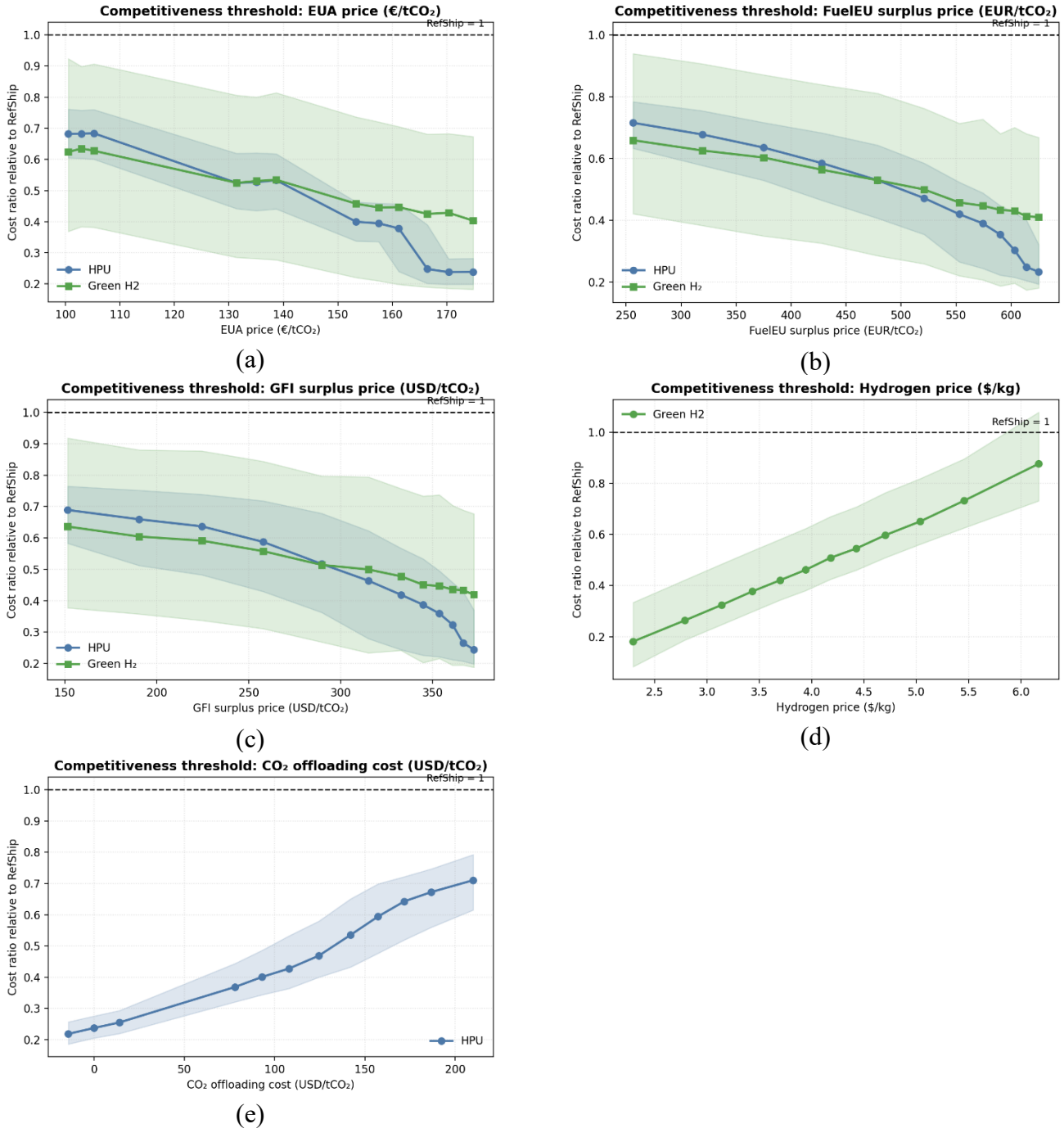


Figure 17. The figure illustrates the sensitivity of lifecycle cost competitiveness to key variables. Simulations are grouped according to the realised value of the variable shown on the x-axis, while all other uncertain variables continue to vary according to their respective stochastic processes. Solid lines represent the median lifecycle cost ratio relative to RefShip, while shaded regions indicate the P10–P90 uncertainty range. Values below unity (RefShip = 1) indicate that the alternative pathway is economically favourable relative to RefShip.

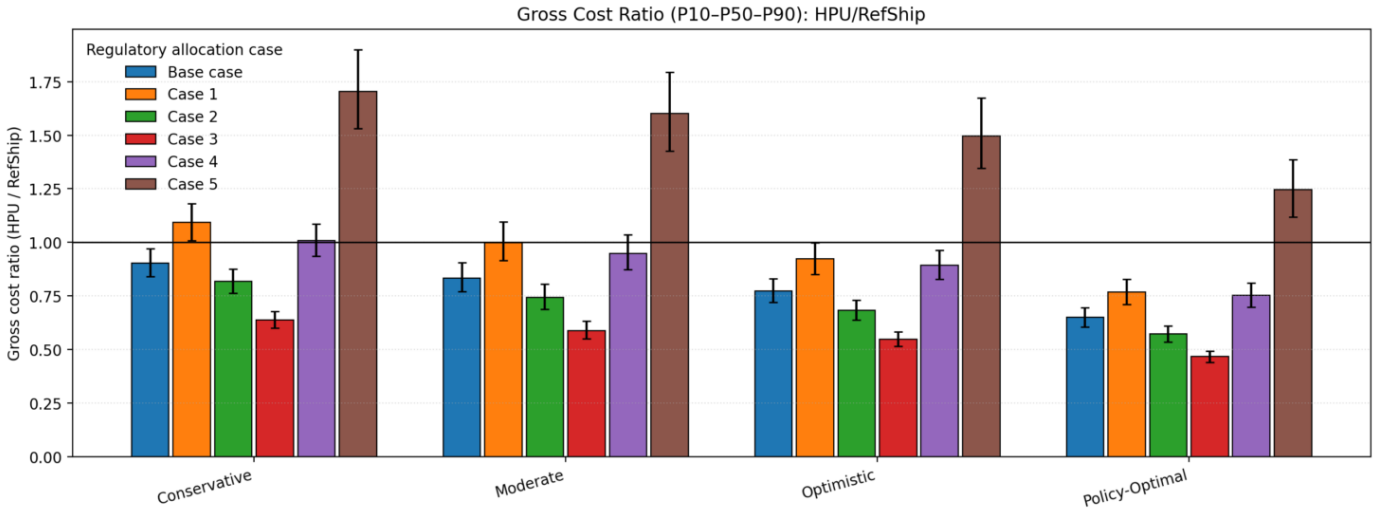
The preceding analyses evaluate cost competitiveness under the base regulatory allocation case, in which a 50:50 non-overlapping allocation between FuelEU Maritime and IMO GFI is assumed for the semi-EU voyage. To assess the robustness of the findings to alternative regulatory exposure conditions, the analysis is extended to six regulatory allocation cases representing different combinations of FuelEU Maritime and IMO

GFI coverage for semi-EU, intra-EU, and non-EU voyage conditions, as summarised in Table 4. Figure 18 compares the gross lifecycle cost ratios of the HPU and Green H_2 pathways relative to RefShip across these cases under the four policy scenarios (Conservative, Moderate, Optimistic, and Policy-Optimal).

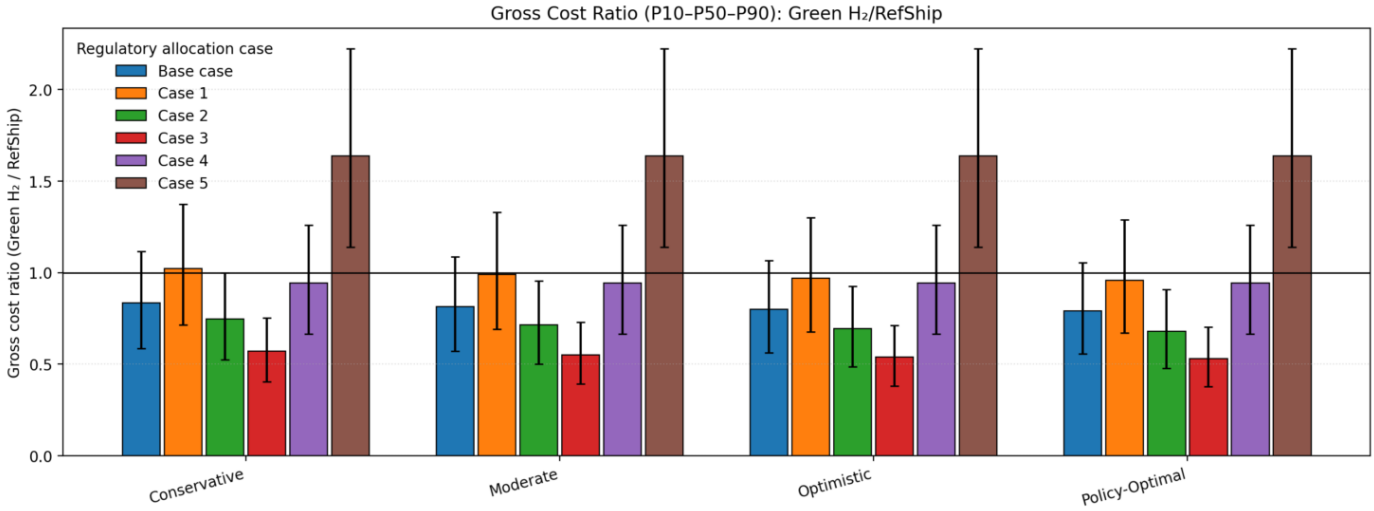
The results show that regulatory coverage materially influences pathway competitiveness, with the absence of both FuelEU Maritime and IMO GFI (**Case 5**) resulting in lifecycle cost ratios above unity and substantially weakening the economic case for both low-emission pathways. Comparatively, HPU exhibits greater sensitivity to regulatory allocation, as reflected by the larger variation in median cost ratios across the cases, whereas Green H_2 shows wider P10–P90 ranges, indicating greater overall economic uncertainty, primarily associated with hydrogen fuel-price variability.

Table 4. Regulatory allocation cases used to evaluate the sensitivity of the selected propulsion pathways to alternative regulatory exposure conditions. The allocation represents the percentage of energy use subject to penalties or rewards under EU ETS, FuelEU Maritime, and IMO GFI. The EU ETS allocation follows the corresponding FuelEU Maritime allocation.

Regulatory allocation case	*Voyage type*	*FuelEU*	*IMO GFI*
Base case	Semi-EU	Include 50%	Include 50%
Case 1	Semi-EU	Include 50%	Include 0%
Case 2	Intra-EU	Include 100%	Include 0%
Case 3	Intra-EU	Include 100%	Include 100%
Case 4	Non-EU voyage	Include 0%	Include 100%
Case 5	Non-EU voyage	Include 0%	Include 0%



(a)



(b)

Figure 18. Sensitivity of gross lifecycle cost ratios to alternative regulatory allocation cases for (a) HPU/RefShip and (b) Green H_2/RefShip under the Conservative, Moderate, Optimistic, and Policy-Optimal scenarios. Six regulatory allocation cases representing different combinations of FuelEU Maritime and IMO GFI exposure for semi-EU, intra-EU, and non-EU voyage conditions are evaluated. Bars represent the median (P50) lifecycle cost ratio, while error bars indicate the P10–P90 uncertainty range. The horizontal line at a cost ratio of unity represents cost parity with RefShip; values below unity indicate economic competitiveness relative to RefShip.

3.4. Discussion on policy and design insights

The results demonstrate that the economic viability of low-carbon maritime propulsion systems cannot be evaluated solely through deterministic lifecycle cost estimates (Section 3.1), as competitiveness is highly dependent on the interaction between fuel-market uncertainty and evolving policy mechanisms. In addition, the analysis in this paper demonstrates that policy is a key mechanism to make the low-carbon pathways economically attractive. The comparison between HPU and Green H_2 pathways reveals two fundamentally different decarbonisation strategies with distinct economic risk structures.

The HPU pathway benefits from a diversified cost structure, where lifecycle cost is distributed across fuel, captured CO_2 management, and policy-linked mechanisms. Although this pathway remains exposed to CO_2 offloading cost and residual emissions penalties, it also gains substantial economic advantages under stringent regulatory environments through FuelEU and IMO GFI surplus-credit mechanisms. The Monte Carlo results indicate that stronger policy ambition progressively shifts the HPU cost distributions toward significantly lower lifecycle cost ratios relative to RefShip. This suggests that carbon pricing and overcompliance-credit trading can substantially improve the financial attractiveness of onboard hydrogen production integrated with carbon capture. In particular, the threshold analysis shows that the competitiveness of HPU strengthens rapidly with increasing EUA price and surplus-credit value, indicating that the pathway is highly policy-sensitive and policy-enhanced. The threshold analysis also concluded that

the HPU stays competitive to RefShip when CO_2 offloading cost does not exceed \$300/tCO_2. However, the strong competitiveness observed under favourable policy scenarios is conditional on the assumed monetisation of FuelEU and IMO GFI surplus credits, whose future trading values, market development, and regulatory interaction remain uncertain.

In contrast, the Green H_2 pathway is less sensitive towards policy strengthening because its lifecycle cost remains overwhelmingly dominated by hydrogen fuel expenditure. Consequently, the economic performance of Green H_2 is governed primarily by future hydrogen supply cost and only secondarily by regulatory incentives. Even under Optimistic and Policy-Optimal scenarios, the reduction in lifecycle cost ratio remains less pronounced than that observed for HPU. The threshold analysis further confirms that Green H_2 becomes economically favourable relative to RefShip only when hydrogen price remains below ~\$5.8/kg, highlighting the critical importance of large-scale low-cost hydrogen production, transportation, and bunkering infrastructure.

The comparison between net and gross lifecycle cost metrics provides additional insight into the role of policy-support mechanisms. When surplus-credit revenues are included, both hydrogen pathways appear economically attractive relative to RefShip, particularly under supportive policy conditions. However, exclusion of FuelEU Maritime and IMO GFI surplus-credit revenues through the gross lifecycle cost analysis substantially reduces the economic performance of Green H_2. The median gross lifecycle cost ratio remains approximately **R = 0.8** across all investigated scenarios, while the upper tail of the distribution extends beyond unity, indicating a non-negligible probability that Green H_2 may remain more expensive than the RefShip under all policy scenarios. In contrast, the economic performance of the HPU pathway improves significantly with increasing policy support. The median gross lifecycle cost ratio decreases from approximately R = 0.90 under the Conservative scenario to R = 0.68 under the Policy-Optimal scenario. Furthermore, the regulatory-allocation sensitivity analysis (Figure 18) reinforces these contrasting risk profiles showing that HPU exhibits greater sensitivity to changes in regulatory coverage, whereas Green H_2 exhibits wider P10-P90 uncertainty ranges, reflecting its stronger exposure to hydrogen-price uncertainty.

The probabilistic framework further demonstrates the importance of uncertainty propagation in long-term maritime investment assessment. Deterministic scenario analysis alone would not capture the wide distribution of possible outcomes observed in the Monte Carlo simulation. In several cases, the upper-bound (P90) gross cost ratios exceed unity despite favourable median values, implying that investors may still face significant downside financial risk under adverse market conditions. This is particularly relevant for Green H_2 pathways, where hydrogen fuel-price volatility dominates overall lifecycle cost uncertainty.

Overall, the findings suggest that future maritime decarbonisation competitiveness will likely be governed by two parallel transitions:

- the development of stringent carbon-pricing and overcompliance-credit systems that reward low-emission operations, and
- the large-scale availability of affordable low-carbon fuels, particularly green hydrogen.

Under supportive policy conditions and high carbon prices, HPU integrated with carbon capture appears capable of achieving substantial economic advantages relative to conventional oil-fuelled shipping. Meanwhile, Green H_2 offers a lower-emission and lower-policy-risk pathway, but its widespread adoption remains strongly constrained by availability of renewable resources and fuel production cost. These findings indicate that future policy frameworks should not only penalise emissions but also accelerate the reduction in low-carbon fuel cost through infrastructure development, supply-chain scaling, and market-support mechanisms.

4. CONCLUSIONS

This study developed a stochastic techno-economic framework to evaluate the lifecycle cost competitiveness of low-carbon maritime propulsion pathways under combined market and policy uncertainty. By integrating Monte Carlo-based fuel-market uncertainty with scenario-conditioned policy pathways, the framework enables probabilistic assessment of lifecycle cost, competitiveness risk, and policy sensitivity for hydrogen-based decarbonisation options.

The results show that both hydrogen pathways can achieve economic competitiveness relative to the conventional MGO-fuelled reference ship under favourable regulatory conditions, although the drivers of competitiveness differ substantially. The HPU route exhibits strong sensitivity to carbon pricing and surplus-credit mechanisms while retaining comparatively robust economic performance across most investigated scenarios. In contrast, Green H_2 competitiveness remains fundamentally constrained by hydrogen fuel cost and depends more strongly on continued policy support and future reductions in hydrogen supply cost. The probabilistic analysis further demonstrates that policy incentives can substantially alter competitiveness outcomes, while uncertainty in fuel and policy conditions remains a major contributor to long-term investment risk.

Overall, the proposed framework provides a scalable approach for integrating price uncertainty, policy dynamics, and lifecycle economics into maritime decarbonisation assessment. The methodology can support future policy evaluation, investment decision-making, and comparative assessment of emerging low-carbon propulsion technologies under evolving regulatory environments. Future work should extend the framework

through incorporation of discounted cash flow analysis for net present value (NPV) evaluation, integration of fuel and EUA index modelling, utilisation of longer-term historical market datasets (if available), inclusion of additional lifecycle cost components, and evaluation of coupled interactions between market, policy, and technology parameters to further improve robustness of long-term maritime decarbonisation assessment. Beyond the pathways examined in this study, the framework can potentially be extended to evaluate other alternative fuels, energy-efficiency technologies, and applied to other vessels with different voyage routes and operational profiles.

ACKNOWLEDGMENTS

For the purpose of open access, the authors have applied a Creative Commons Attribution (CC BY) license to any Author Accepted Manuscript version arising from this submission.

FUNDING DECLARATION

This research project is part of the CREATE Thematic Programme in Decarbonisation and is supported by the National Research Foundation, Prime Minister's Office, Singapore under its Campus for Research Excellence and Technological Enterprise (CREATE) programme.

AUTHORSHIP CONTRIBUTIONS

All authors led the conceptualisation. L.C. Law led the methodology development. All authors provided key inputs. L.C. Law led manuscript preparation, performed the analysis, prepared tables and figure, and wrote the main manuscript text. All authors reviewed the manuscript. E. Mastorakos arranged funding. All authors read and approved the final version.

CONFLICT OF INTEREST

The authors declare that they have no known competing financial interests or personal relationships that could have appeared to influence the work reported in this paper.

REFERENCES

[1] G. H. Park, S. Hong, S. Percy and S. W. Kim, “Techno-economic feasibility study of imported green hydrogen via inter-continental route: From Australia to South Korea,” *Applied Energy,* vol. 397, p. 126288; https://doi.org/10.1016/j.apenergy.2025.126288, 2025.

[2] L. C. Law, E. Mastorakos and S. Evans, “Estimates of the Decarbonization Potential of Alternative Fuels for Shipping as a Function of Vessel Type, Cargo, and Voyage,” *Energies,* vol. 15, no. 7468, p. https://doi.org/10.3390/en15207468, 2022.

[3] J. R. Smith, S. Gkantonas and E. Mastorakos, “Modelling of Boil-Off and Sloshing Relevant to Future Liquid Hydrogen Carriers,” *Energies,* vol. 15, no. 6, p. https://doi.org/10.3390/en15062046, 2022.

[4] F. Bianchi, M. Pero and M. Rossi, “Transitioning the European maritime industry to hydrogen: a system's perspective for policy making,” *Energy Policy,* vol. 214, p. 115259; https://doi.org/10.1016/j.enpol.2026.115259, 2026.

[5] A. Sola, R. Rosa and A. M. Ferrari, “Green Hydrogen and Its Supply Chain. A CriticalAssessment of the Environmental Impacts,” *Advanced Sustainable Systems,* vol. 9, p. 2400708; https://doi.org/10.1002/adsu.202400708, 2025.

[6] imarc, “Green Hydrogen Prices, Trend, Chart, Demand, Market Analysis, News, Historical and Forecast Data Report 2026 Edition,” imarc, April 2026. [Online]. Available: https://www.imarcgroup.com/green-hydrogen-pricing-report. [Accessed 4 May 2026].

[7] S. Kheirani, A. Houmani and M. H. Jahangir, “Economical Investigation of green hydrogen supply for Hydrogen-Powered ship by Off-Grid wave and wind energy hubs,” *Energy Conversion and Management: X,* vol. 26, p. 101006; https://doi.org/10.1016/j.ecmx.2025.101006, 2025.

[8] J. Kim, E. Lee, H. T. T. Vu, K. Lee, H. Kim, J. Choi, J. Han, K. Park, J. Kim, B. Choi, H. Park and D. Chang, “Economic analysis of intercontinentally shipped green liquid hydrogen based on basic design of facilities in supply chain,” *International Journal of Hydrogen Energy,* vol. 113, p. 39–49; https://doi.org/10.1016/j.ijhydene.2025.02.415, 2025.

[9] Ship & Bunker, “Rotterdam Bunker Prices,” Ship & Bunker, 6 May 2025. [Online]. Available: https://shipandbunker.com/prices/emea/nwe/nl-rtm-rotterdam#VLSFO. [Accessed 5 May 2026].

[10] Z. Chen, Y. Zhao, X. Zheng, G. Shao, Y. Li, M. Liu, J. Shi and C. Gu, “The impacts of the hydrogen economy on climate: Current research and future projections to 2050,” *International Journal of Hydrogen Energy,* vol. 119, pp. 204-217; https://doi.org/10.1016/j.ijhydene.2025.03.230, 2025.

[11] L. C. Law, E. Mastorakos, M. R. Othman and A. Trakakis, “A thermodynamics model for the assessment and optimisation of onboard natural gas reforming and carbon capture,” *Emission Control Science and Technology,* no. https://doi.org/10.1007/s40825-023-00234-z, 2023.

[12] L. C. Law, S. Gkantonas, A. Mengoni and E. Mastorakos, “Onboard pre-combustion carbon capture with combined-cycle gas turbine power plant architectures for LNG-fuelled ship propulsion,” *Applied Thermal Engineering,* vol. 248, no. https://doi.org/10.1016/j.applthermaleng.2024.123294, 2024.

[13] S. Kim, S. Oh and S. Kang, “Techno-economic assessment of liquefied hydrogen tanker ships utilizing various propulsion systems,” *Energy Conversion and Management,* vol. 336, p. https://doi.org/10.1016/j.enconman.2025.119895, 2025.

[14] W. Schreuder, J. C. Slootweg and B. v. d. Zwaan, “Techno-economic assessment of low-carbon ammonia as fuel for the maritime sector,” *Applications in Energy and Combustion Science,* vol. 22, p. 100330; https://doi.org/10.1016/j.jaecs.2025.100330, 2025.

[15] H. Kim and S. Park, “Ship investment patterns and performance: A comparative analysis of Greece, South Korea, China, and Japan,” *Transportation Research Interdisciplinary Perspectives,* vol. 31, p. 101415; https://doi.org/10.1016/j.trip.2025.101415, 2025.

[16] A. N. Alkhaledi, S. Sampath and P. Pilidis, “Economic analysis of a zero-carbon liquefied hydrogen tanker ship,” *International Journal of Hydrogen Energy,* vol. 47, p. https://doi.org/10.1016/j.ijhydene.2022.06.168, 2022.

[17] H. Jeong and H. Yun, “A stochastic approach for economic valuation of alternative fuels: The case of container ship investments,” *Journal of Cleaner Production,* vol. 418, p. 138182; https://doi.org/10.1016/j.jclepro.2023.138182, 2023.

[18] S. Park, H. Lee and D. Kim, “Regulatory compliance and operational efficiency in maritime transport: Strategies and insights,” *Transport Policy; https://doi.org/10.1016/j.tranpol.2024.06.024,* vol. 155, pp. 161-177; , 2024.

[19] B. A. Zincir and B. Zincir, “Fleet-scale evaluation of ammonia and hydrogen pathways under EU ETS and FuelEU Maritime regulations,” *International Journal of Hydrogen Energy,* vol. 203, p. 153115; https://doi.org/10.1016/j.ijhydene.2025.153115, 2026.

[20] K. Singh and S. Viswanathan, “Techno-economic modelling of liquid hydrogen tankers: Capex, Opex, scale economies, and emission trade-offs,” *International Journal of Hydrogen Energy,* vol. 204, p. 153259; https://doi.org/10.1016/j.ijhydene.2025.153259, 2026.

[21] J. Ahn, J. Lee, Y. Yun, J. E. Park and K. Lee, "Financed emissions and climate alignment of an LNG carrier with regard to investment portfolio achieving net-zero for international shipping," *Energy Reports,* vol. 15, p. 109269; https://doi.org/10.1016/j.egyr.2026.109269, 2026.

[22] C. To, "FuelEU abatement methodologies driving a new market in compliance surplus trading," S&P Global, 2026. [Online]. Available: https://www.spglobal.com/energy/en/news-research/blog/energy-transition/081825-fueleu-abatement-methodologies-driving-a-new-market-in-compliance-surplus-trading. [Accessed 2 August 2026].

[23] F. Spiegelenberg, "IMO policy measures: Ensuring certainty for shipping's energy transition," Global Maritime Forum, 27 March 2025. [Online]. Available: https://globalmaritimeforum.org/insight/imo-policy-measures-ensuring-certainty-for-shippings-energy-transition/. [Accessed 2 August 2026].

[24] Lloyd's Register, "IMO Marine Environment Protection Committee (MEPC 83): Summary Report," April 2025. [Online]. Available: https://maritime.lr.org/MEPC-83-Summary-Report?_gl=1*grsa4n*_gcl_au*MTk5OTI0Njc5MC4xNzg0NTI5MTk5*_ga*ODAyNTE2MjMuMTc4NDUyOTIwMA..*_ga_BTRFH3E7GD*czE3ODYzNTM3OTAkbzYkZzAkdDE3ODYzNTM3OTAkajYwJGwwJGg5MzkxNTQxMTE.. [Accessed 10 April 2026].

[25] L. C. Law, N. Tsoulakos, E. Meristoudi, P. Theodossopoulos and E. Mastorakos, "Data-driven decarbonisation strategies for ships, part 1: Technical feasibility and emissions modelling," *Energy Reports,* vol. 16, p. https://doi.org/10.1016/j.egyr.2026.109610, 2026.

[26] L. C. Law, N. Tsoulakos, E. Meristoudi, P. Theodossopoulos and E. Mastorakos, " Data-Driven Decarbonisation Strategies for Ships, Part 2: Financial Projections," *Energy Reports,* p. Accepted for publication., 2026.

[27] L. C. Law, M. R. Othman and E. Mastorakos, "Numerical analyses on performance of low carbon containership," *Energy Reports,* vol. 9, pp. 3440-3457; https://doi.org/10.1016/j.egyr.2023.02.035, 2023.

[28] M. S. A. Towhid and S. B. Hossain, "Advances and challenges in cryogenic liquefied hydrogen (LH2) maritime transportation: Thermal performance, tank design, boil-off gas management, and techno-economic considerations," *Renewable and Sustainable Energy Reviews,* vol. 233, p. 116850; https://doi.org/10.1016/j.rser.2026.116850, 2026.

[29] National Renewable Energy Laboratory, "Life Cycle Greenhouse Gas Emissions from Solar Photovoltaics," 2012. [Online]. Available: https://www.nrel.gov/docs/fy13osti/56487.pdf. [Accessed 24 April 2025].

[30] D. Nugent and B. K. Sovacool, "Assessing the lifecycle greenhouse gas emissions from solar PV and wind energy: A critical meta-survey," *Energy policy,* vol. 65, pp. 229-244, 2014; http://dx.doi.org/10.1016/j.enpol.2013.10.048.

[31] L. C. Law, B. Foscoli, E. Mastorakos and S. Evans, "A Comparison of Alternative Fuels for Shipping in Terms of Lifecycle Energy and Cost," *Energies,* vol. 14, no. 24, p. https://doi.org/10.3390/en14248502, 2021.

[32] D. Kundu, A. Barathi, K. Pooja, M. Surya, S. Jacob, A. Koley, P. Samanta, V. Kumar, A. D. Chintagunta, N. S. S. Kumar, S. Balachandran and H. Singh, "Green hydrogen pathways for a net-zero future: technologies, circular economy integration, life-cycle performance and safety dimensions," *Royal Society of Chemistry,* vol. 16, no. 15, pp. 13471-13514, 2026; https://doi.org/10.1039/d5ra09599a.

[33] Baker Hughes, "NovaLT™16 gas turbine (17.5 MW, 50/60 Hz)," Baker Hughes, 7 June 2026. [Online]. Available: https://www.bakerhughes.com/gas-turbines/novalt-technology/novalt16. [Accessed 2026].

[34] A. Abuzayed, M. G. Pollitt, M. Liebensteiner and S. Hochgreb, "Exploring the feasibility of low-carbon fuel blends in CCGTs for deep decarbonization of power systems," *Energy Strategy Reviews,* vol. 63, p. 102036; https://doi.org/10.1016/j.esr.2026.102036, 2026.

[35] Ipieca, "Combined-cycle gas turbines," Ipieca, November 2022. [Online]. Available: https://www.ipieca.org/resources/energy-efficiency-compendium/combined-cycle-gas-turbines-2022. [Accessed 8 June 2026].

[36] S. Zhu, Z. Ma, K. Zhang and K. Deng, "Energy and exergy analysis of a novel steam injected turbocompounding system applied on the marine two-stroke diesel engine," *Energy Conversion and Management,* vol. 221, p. https://doi.org/10.1016/j.enconman.2020.113207, 2020.

[37] vCalc, "Haversine - Distance," vCalc, 12 December 2025. [Online]. Available: https://www.vcalc.com/wiki/vcalc/haversine-distance?viewer=code. [Accessed 1 April 2026].

[38] European Parliament and the Council of The European Union, "REGULATION (EU) 2023/1805 OF THE EUROPEAN PARLIAMENT AND OF THE COUNCIL on the use of renewable and low-carbon fuels in maritime transport, and amending Directive 2009/16/EC," Official Journal of the European Union, European, 13 September 2023.

[39] A. M. T. Alzayedi and S. S. a. P. Pilidis, "Techno–Economic and Risk Evaluation of Combined Cycle Propulsion Systems in Large Container Ships," *Energies,* vol. 15, p. https://doi.org/10.3390/en15145178, 2022.

[40] Y. W. Ryu, S. Yun, S.-H. Kim, S. H. Yun, H. Kim, J. T. Jang and J. Park, "Multi-objective optimization of combined steam and dry reforming for low-carbon hydrogen production: Balancing techno-economic performance and

environmental sustainability," *International Journal of Hydrogen Energy,* vol. 236, p. 155123; https://doi.org/10.1016/j.ijhydene.2026.155123, 2026.

[41] IMO, "Resolution MEPC.376(80) Guidelines on Life Cycle GHG Intensity Gof Marine Fuels (LCA Guidelines)," 7 July 2023. [Online]. Available: https://wwwcdn.imo.org/localresources/en/KnowledgeCentre/IndexofIMOResolutions/MEPCDocuments/MEPC.376(80).pdf. [Accessed 29 November 2023].

[42] P. Ellersdorfer, M. H. A. Khan, M. Lejeune, A. Kerwick, T. Nolan, J. G. Martinez, A. Darling, I. MacGill and R. Daiyan, "Navigating green Seas: An open-source tool for costing the development of green shipping corridors," *Fuel,* vol. 410, p. https://doi.org/10.1016/j.fuel.2025.137870, 2026.

[43] S. Lee, "Mastering Wiener Process in Stochastic Processes, A Comprehensive Guide to Understanding and Applying Wiener Process Concepts," Number Analytics, 11 June 2025. [Online]. Available: https://www.numberanalytics.com/blog/ultimate-guide-wiener-process-stochastic-processes. [Accessed 1 April 2026].

[44] D. Cicmilović, "Hidden Markov Model for correlated Ornstein–Uhlenbeck observations and application to gasoline prices forecasting," *Communications in Nonlinear Science and Numerical Simulation,* vol. 143, p. 108630; https://doi.org/10.1016/j.cnsns.2025.108630, 2025.

[45] H. Pei, "Mean-Reverting Spread Modeling: Caveats in Calibrating the OU Process," Hudson and Thames, [Online]. Available: https://hudsonthames.org/caveats-in-calibrating-the-ou-process/. [Accessed 14 May 2026].

[46] Y. Akbay, "Energy and Commodity Prices with Mean-Reverting Models, A Practical Guide for Quantitative Analysts," Medium, 21 September 2025. [Online]. Available: https://medium.com/@yavuzakbay/energy-and-commodity-prices-with-mean-reverting-models-376610014a48. [Accessed 14 May 2026].

[47] Ship & Bunker, "Rotterdam Bunker Prices," Ship & Bunker, 13 May 2026. [Online]. Available: https://shipandbunker.com/prices/emea/nwe/nl-rtm-rotterdam#MGO. [Accessed 15 May 2026].

[48] Engine, "Fuel Switch Snapshot: Hormuz closure sends bunker prices soaring in major ports," Engine, 10 March 2026. [Online]. Available: https://www.engine.online/news/fuel-switch-snapshot-hormuz-closure-sends-bunker-prices-soaring-in-major-ports-7869. [Accessed 16 May 2026].

[49] Seaboard Marine, "Bunker Increase (All Markets) and U.S. Domestic Fuel Surcharge Update," Seaboard Marine, 2 April 2026. [Online]. Available: https://www.seaboardmarine.com/customer-advisories/bunker-increase-all-markets-and-u-s-domestic-fuel-surcharge-update/. [Accessed 16 May 2026].

[50] Pamelakarmelita, "Introduction to Monte Carlo Simulation with Geometric Brownian Motion," Medium, 9 September 2024. [Online]. Available: https://medium.com/@pamelakarmelita/introduction-to-monte-carlo-simulation-with-geometric-brownian-motion-c4a5e3f07ad1. [Accessed 14 May 2026].

[51] ABN.AMRO, "ESG Economist - Scenarios shaping EU ETS prices," ABN.AMRO, 16 September 2025. [Online]. Available: https://www.abnamro.com/research/en/our-research/esg-economist-scenarios-shaping-eu-ets-prices. [Accessed 10 May 2026].

[52] C. Ekai, "Three-Point Estimation in Risk Management: PERT, Triangular, and When to Use Each Triangular, and When to Use Each," 24 March 2026. [Online]. Available: https://riskpublishing.com/three-point-estimation-in-risk-management-pert/. [Accessed 2 August 2026].

[53] D. Johnson, "The triangular distribution as a proxy for the beta distribution in risk analysis," *Journal of the Royal Statistical Society,* vol. 46, no. 3, pp. 387–398; https://doi.org/10.1111/1467-9884.00091, 1997.

[54] J. Edmonds, C. Nichols, M. Adamantiades, J. Bistline, J. Huster, G. Iyer, N. Johnson, P. Patel, S. Showalter, N. Victor, S. Waldhoff, M. Wise and F. Wood, "Could congressionally mandated incentives lead to deployment of large-scale CO2 capture, facilities for enhanced oil recovery CO2 markets and geologic CO2 storage?," *Energy Policy,* vol. 146, p. 111775; https://doi.org/10.1016/j.enpol.2020.111775, 2020.

[55] S&P Global, "Platts Global Bunker Cost Calculator," S & P Global, March 2026. [Online]. Available: https://www.spglobal.com/energy/en/news-research/infographics/content-design-infographics/platts-global-bunker-cost-calculator. [Accessed 10 May 2026].

[56] Homaio, "European Union Allowances|EUA," Homaio, May 2026. [Online]. Available: https://app.homaio.com/market/EUA_DAILY. [Accessed 10 May 2026].

[57] A. Hatta, C. Consoli and M. Seyyedi, "Cost of CO2 Storage," December 2025. [Online]. Available: https://www.globalccsinstitute.com/wp-content/uploads/2025/12/Cost-of-CO2-Storage-1225.pdf. [Accessed 1 April 2026].

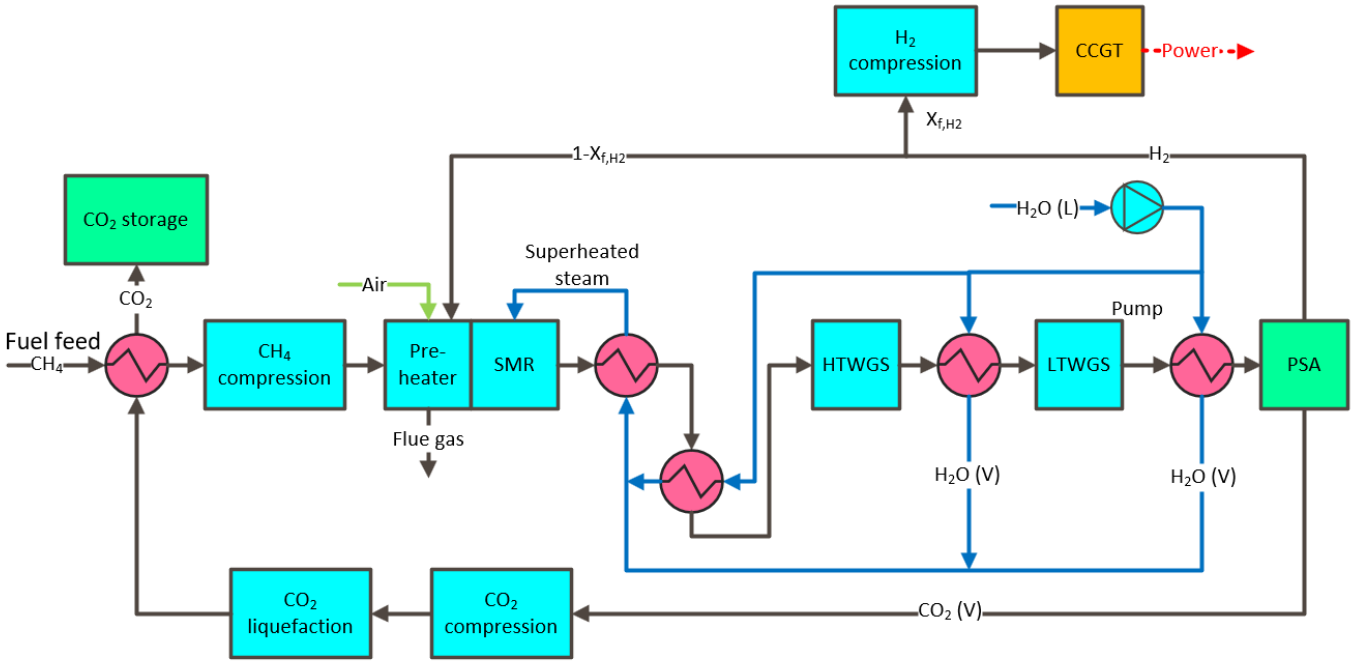
[58] N. Beckert, "CCS: transportation and storage likely to be even more expensive than expected," Tanle.Briefings, 19 February 2026. [Online]. Available: https://table.media/en/climate/news-en/ccs-transportation-and-storage-likely-to-be-even-more-expensive-than-expected. [Accessed 10 May 2026].

[59] R. Babaei, D. S.-K. Ting and R. Carriveau, “Decarbonizing maritime logistics through hydrogen-powered container ships,” *Renewable Energy Focus,* vol. 57, p. 100823; https://doi.org/10.1016/j.ref.2026.100823, 2026.

[60] A. Navarrete and Y. Zhou, “The price of green hydrogen: How and why we estimate future production costs,” the International Council on Clean Transportation, 20 May 2024. [Online]. Available: https://theicct.org/the-price-of-green-hydrogen-estimate-future-production-costs-may24/. [Accessed 2 August 2026].

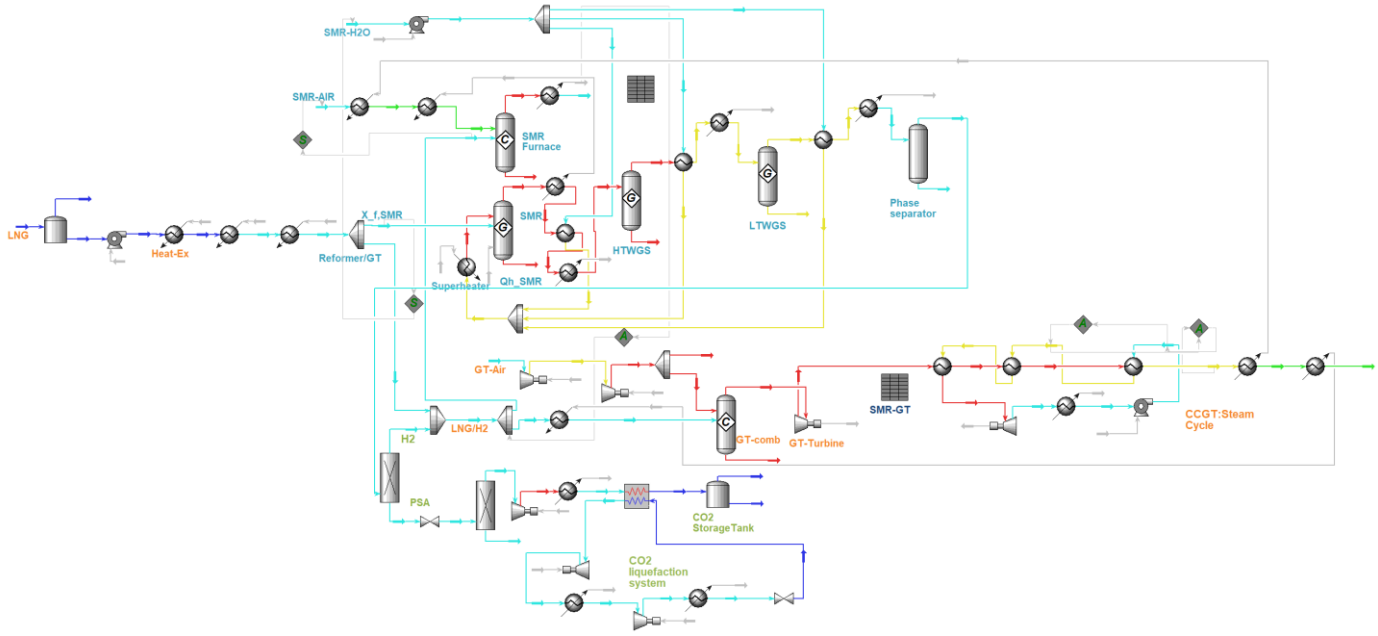
[61] Marine Public, “Ultimate Ship LNG Bunkering Checklist and Safety Guide,” 20 January 2026. [Online]. Available: https://www.marinepublic.com/blogs/oil-and-gas/453889-ultimate-ship-lng-bunkering-checklist-and-safety-guide. [Accessed 20 May 2026].

Appendix A: Aspen simulation of hydrogen production unit (HPU) model used to produce renewable hydrogen onboard.



[1]

(a)



(b)

Figure A1. (a) Simplified Aspen HYSYS process flow diagram and (b) Aspen HYSYS model of the onboard hydrogen production unit based on steam methane reforming (HPU). Methane fuel is assumed stored onboard at -162 ℃ at atmospheric pressure. The methane is compressed to 25 bars before entering the reforming system. The compressed methane is preheated and subsequently converted through steam reforming (SMR), followed by high-temperature and low-temperature water–gas shift reactions (HTWGS and LTWGS). The produced synthesis gas is purified using pressure swing adsorption (PSA) to obtain high-purity hydrogen, while the by-product CO_2 is compressed and liquefied using an external refrigeration cycle for onboard storage and offshore discharge. Potential cold-energy recovery from the cryogenic methane stream and CO_2 liquefaction process may further improve overall system efficiency. However, cold-energy integration is not considered in the present study. The integrated system also includes hydrogen compression prior to utilisation in the onboard combined cycle gas turbine (CCGT) power system.

Table A2. Key inputs for the onboard hydrogen production unit based on steam methane reforming (HPU). The process simulation and optimisation were conducted using Aspen HYSYS.

Input parameter	*Normalised value*	*Sources*
Feedstock	LNG (assumed 100% methane), -162°C, 1 bar	Literature [61]
Seawater condition	25°C, 1 bar	Assumption
Production process & condition	1. LNG vaporisation & compression (to 25 bar) 2. Steam methane reforming 3. HT water gas shift (500°C) 4. LT water gas shift (165°C) 5. H_2 purification and compression using PSA 6. CO_2 compression and liquefaction (-20°C, 20 bar)	Aspen simulated
Steam to fuel ratio	~3.163	Aspen optimised [11]
Furnace fuel source	Hydrogen product	Aspen optimised
Product	H_2 (also known as reformate), CO_2	Aspen simulated

Table A3. Key optimised process parameters for the onboard hydrogen production unit based on steam methane reforming (HPU). The process simulation and optimisation were conducted using Aspen HYSYS for three different feedstock composition including methane (CH_4), liquefied natural gas (LNG), and boil-off gas (BOG).

Simulated parameter	*Case 1 (CH_4)*	*Case 2 (LNG)*	*Case 3 (BOG)*	*Sources*
Feedstock composition (mole %)	CH_4: 100%	CH_4: 95.7% N_2: 0.4% C_2H_6: 3.2% C_3H_8: 0.6% C_4H_{10}: 0.1%	CH_4: 91.8% N_2: 8.2%	Assumption
LNG consumption ($kgLNG/kgH_2$)	2.33	2.31	2.27	Aspen simulated
Water consumption (kgH_2O/kgH_2)	8.28	7.87	7.32	Aspen simulated
Electricity demand ($kWhe/kgH_2$)	0.88	0.86	0.76	Aspen simulated
Included electricity consumers	1. NG compression: ~30 kWhe/tLNG (Aspen) 2. CO_2 compression and liquefaction: ~130 kWhe/tCO_2 (Aspen) 3. Auxiliary pumps: ~20 kWhe/tLNG (Aspen) 4. H_2 product compression (if required)			Aspen simulated
CO_2 captured rate ($kgCO_2/kgH_2$)	5.86		4.99	Aspen simulated
Reformate lower heating value (kJ/kg)	93,900	90,850	77,060	Aspen simulated
Reformate composition (mole %)	CH_4: 0.20% H_2: 97.80% CO: 1.60% CO_2: 0.23% H_2O: 0.17%	CH_4: 0.22% H_2: 97.45% CO: 1.84% CO_2: 0.23% H_2O: 0.17%	CH_4: 0.17% H_2: 95.91% CO: 1.33% CO_2: 0.23% H_2O: 0.17%	Aspen simulated

Appendix B: Ship performance simulation for reference ship (RefShip) and ship integrated with hydrogen production unit (HPU) model

In the ship performance simulation, a typical ship operational profile with assumption on the percentage of time spent at different operational modes (laden, ballast, loading, unloading, drifting, and idling) and sailing speeds was used. With this, the propulsion system was operated to meet the power demand of the ship at different speeds. The engine loads and operational hour of CCGT or 2-stroke engine and the auxiliary engines were summed.

From the power demand, the hourly total energy consumed was obtained. Based on this information, the total amount of fuel consumed (ton/year), total CO_2, CO_2eq and WTW CO_2eq emissions (ton/year), and the total CO_2 captured by the HPU model were calculated. By using this calculated output, the Carbon Intensity Indicator (CII) and Greenhouse Gas Fuel Intensity (GFI) values were calculated by using the formula provided by the European Council and IMO, Equations (19 – 22). CII is estimated by dividing the Tank-to-Wake (TTW) emissions with deadweight and distance travelled, Eq. (19). For GFI, it is estimated as the sum of the TTW and WTT emissions in the unit of gCO_2eq/MJ, Equation (22), where the WTT emissions factor is obtained from Table 1 and TTW emission factor is calculated from Equation (20 – 21).

$$CII = \frac{TTW\ CO_2(gCO2)}{deadweight\ (tons) \times distance\ travelled\ (nm)} \tag{19}$$

$$TTW\ CO_{2eq}(gCO2eq) = (\mathrm{GWP_{CO2}} \times C_{f,CO2} + \mathrm{GWP_{CH4}} \times C_{f,CH4} + \mathrm{GWP_{N2O}} \times C_{f,N2O}) \tag{20}$$

$$TTW\ (\frac{gCO2eq}{MJ}) = \frac{\Sigma TTW\ CO_{2eq}(gCO2eq)}{m_{fuel} \times LHV} \tag{21}$$

$$GFI = GHG_{WTW}\ (\frac{gCO2eq}{MJ}) = GHG_{WTT}(\frac{gCO2eq}{MJ}) + GHG_{TTW}(\frac{gCO2eq}{MJ}) \tag{22}$$

With the estimated CII and GFI values, the FuelEU Maritiem and IMO GFI penalties and surplus were calculated. The FuelEU penalty was calculated by using Equation (23), as given in the official journal of the European Union 2023/1805. The values 41,000 and 2,400 in the equation are the equivalent LHV of one metric ton of VLSFO, and the amount paid in EUR per equivalent metric ton of VLSFO. The percentage of taxable E_{fuel} is considered as 50% for voyages between EU and non-EU ports, and 100% for voyages between two EU ports.

$$Fuel\ EU\ Penalty, FUEP\ (\$) = \frac{|Compliance\ Balance|}{GHGIE_{actual} \times 41000} \times 2400 \times \frac{1.0849\ USD}{EUR} \times \%\ taxable\ MJ \tag{23}$$

During Marine Environment Protection Committee (MEPC) 83 in 2025, the IMO has also introduced a system to penalise emissions exceeding the GFI compliance targets. Two annual GFI targets are defined: the Base Target (GFI_{Base}) and the Direct Compliance Target ($GFI_{Direct\ Compliance}$). The difference between the Direct Compliance Target and the Base Target is the Tier 1 Compliance Deficit, penalised at \$100/ton CO_2eq; and the difference between Base target and attained annual GFI is known as Tier 2 Compliance Deficit (or Compliance Surplus), penalised at \$380 /ton CO_2eq. Tier 2 deficits can also be balanced using surplus units banked from previous years or transferred between ships within the same year. Eqs. (24) and (25) are used to determine the level of remediation required for negative compliance, by multiplying the difference in the GFI targets and attained values with the taxable % of energy consumed E_{fuel} and the rate of penalties.

$$Tier\ 1\ Penalty\ (\$) = \left(GFI_{Direct\ Compliance} - GFI_{Base}\right) \times E_{fuel} \times \frac{\$100}{ton\ CO_2} \tag{24}$$

$$Tier\ 2\ Penalty\ (\$) = (GFI_{Base} - GFI_{attained}) \times E_{fuel} \times \frac{\$380}{ton\ CO_2} \tag{25}$$